IRIS BASED BIOMETRIC SYSTEM FOR HUMAN IDENTIFICATION

A dissertation Submitted in partial fulfillment of the requirements
for the award of the degree of

MASTER OF ENGINEERING
(Computer Technology & Applications)

By
Gashaw Ayalew Feyisa
College Roll No. 29/CTA/03
Delhi University Roll No. 8521

Under the guidance of
Prof. Goldie Gabrani

Department Of Computer Engineering
Delhi College of Engineering
Bawana Road, Delhi-110042
(University of Delhi)
June 2006

Certificate

I hereby certify that the work which is being presented in the dissertation entitled "**IRIS BASED BIOMETRIC SYSTEM FOR HUMAN IDENTIFICATION**", which is submitted by **Gashaw Ayalew Feyisa,** in the partial fulfillment of the requirements for the award of the degree of Master of Engineering in Computer Technology and Applications, Department of Computer Engineering, Delhi College of Engineering, Delhi.

This is to certify that the above statement made by the candidate is true to the best of my knowledge.

Prof. Goldie Gabrani
(Head of Department)
Computer Engineering Department,
Delhi College of Engineering,
(Project Guide)
Signature:_____

Abstract

There is an increase in security concerns in security concerns on issues such as identity theft indicates the needs of a new reliable security system. This can be accomplished by using biological features of Human via Biometrics such as Iris recognition. In the first place, these thesis review literature on Iris scan Technology comparing it with other image based biometrics. The first aim of implementing this project is to reconstruct an iris recognition system for Near Infrared (NIR) image based on the Daugman's algorithm. After finishing this, the second aim is to extend the finished system to handle color spectrum image and improved on individual sections. Daugman's iris recognition system is based on the location of the iris boundaries via a circular edge detector utilizing integrodifferential operators. The iris is then normalized using a rubber sheet model. After projecting onto Gabor filters, phase information is extracted and stored in a bit code. Hamming distances between the input image code and stored codes are calculated. Based on a test of statistical independence the irises are matched or not. Noisy areas of the iris are masked off from analysis via mask bits. Combining these elements an iris recognition system was implemented. The system produced in this project was written in Matlab. The database used in this project is from CASIA and UBIRIS, only around 70-80% can locate the iris correctly by the program developed in this project. Out of those images, about 75% of them can be recognized correctly without accepting any false matches. Therefore, the iris recognition system developed in this project was partly successfully. The failure to recognize all color images is because of the poor localization and designing the Gabor filter parameters using a small database. However, the system has a good processing time on comparing the irises.

[Key Words: *Iris, Iris Recognition, Identification, Iris scan, Biometrics, Image based biometrics, pattern recognition, Daugman's Algorithm, Image processing.*]

Acknowledgement

Success in life is never attained single handedly. I would like to express my heartfelt gratitude to my **God** almighty that revealed Himself to me through the Holy Spirit and has since been my source of strength and wisdom.

My sincere appreciation and thanks goes to my Project supervisor and head of department, **Prof. Goldie Gabrani** for the professional guidance and inspiration that has enabled me carry out this research.

I also wish to extend my earnest thanks to the Department of computer engineering staff members and Delhi College of Engineering community. Special thanks to my instructors namely: **Prof. D. Roy Choudhury**, **Prof. Ashok Dey, Dr. S. K. Saxena**, **Mrs. Rajni Jindal** and **Mr. Rajeev Kumar** for their support, encouragement and for teaching me.

I'd like to thank **CASIA** and **UBIRIS** – for the importantly iris database, these organizations make available to impoverished students. Prof. John Daugman – for basically fathering iris recognition .

I am deeply grateful to thank all my classmates on the computer engineering program for having made my academic and social life comfortable at DCE

Lastly, my **dad**, **mom**, **sisters** and **brother** for patiently waiting, support and understanding me.

MAY GOD BLESS YOU ABUNDANTLY

Gashaw Ayalew Feyisa
M.E. (Computer Technology & Applications)
College Roll No. 29/CTA/03
University Roll No. 8521

Table of contents

1. Introduction 8

2. Background and Project Overview 10

2.1 Introduction 10

2.2 What is Biometric? 10

2.3.1 Face 13
2.3.2 Fingerprints 15
2.3.3 Hand geometry 17
2.3.4 Hand veins 20
2.3.5 Iris 23
2.3.6 Retina 26
2.3.7 Signature 28

2.4 Multiple biometric 32

2.5 Iris Recognition 34

2.6 Project Overview 35

2.7 Programming Language 35

3. Theory that governs Iris Recognition 37

3.1 Anatomy and Physiology of the Iris 37

3.2 Iris Recognition 39

3.3 Daugman's Algorithm 40

3.3.1 Overview of the algorithm 40
3.3.2. Location of the Iris 43
3.3.3 Normalization of the Iris Image 43
3.3.4 Projection onto a Gabor Filter and Generation of the Iris Code 44
3.3.5 Generation of Mask Bits 46
3.3.6 Comparison of Iris Codes to Determine Identity 46
3.3.7 Accuracy of the System 47

3.4 The Iris Databases 47

3.4.1 CASIA 47
3.4.2 UBIRIS 48

3.5 Other Iris Recognition Systems 49

4. Implementation 50

4.1 Location of the eye Socket 50

4.2 Localizing Pupil and Iris 51

4.2.1 Algorithm to find the pupil 55
4.2.2 Algorithm to find the Iris 56
4.2.3 Verifying the Estimate Center 59

4.3 Finding the bottom curve 63

4.5 Normalizing the Image 64

4.6 Mask Bit Generation 65

4.7 Filtering with Gabor 68

4.8 Comparing Codes 69
2.9 Shifting 71
5. Results and discussion 72
6. Conclusion 75
7. Future Development 77
7.1 Filter Design and Localization Improvements 77
7.2 Automated Eye Socket Detection 77
7.3 Real Time System 77
7.4 Implementation Using Other Programming Language 78
7.5 Improvements on Color Visible Spectrum Database 78
References: 79

List of Figures

Figure 2-1 Generalized biometric system 11
Figure 2-2 Minutiae, ridge endings and ridge bifurcations 15
Figure 2-3 Typical fingerprint feature extraction algorithm 16
Figure 2-4 The ROC curve comparison 17
Figure 2-5 Prototype design a) Platform Placement Photograph taking 18
Figure 2-6 Location of measurement point for feature extraction 19
Figure 2-7 Schematic of imaging unit 21
Figure 2-8 Original captured image, and vein structure after prune the medial axis 22
Figure 2-9 (a) Iris image (b) localization (c) unwrapped (d) enhancement 23
Figure 2-10 a) Daugman system, top 8 circular band, iris code & demodulation 24
Figure 2-11 Retinal scanned image 27
Figure 2-12 Quantities for testing curvilinear bands 28
Figure 2-13 Proposed approach versus global thresholding 28
Figure 2-14 a) Directional matrix b) Signature c) direction vector 30
Figure 2-15 Function x(t) after wavelet transform 31
Figure 2-16 Cost vs. accuracy 33
Figure 3-1The cross section of the Iris 37
Figure 3-2 Flow Chart of Basic Implementation of Daugman's Algorithm. 42
Figure 3-3 Boundaries forms of Occlusion from Eyelids, Eyelashes, & Reflections43
Figure 3-4 The Real Component of a Gabor filter 45
Figure 3-5 Image capture framework 48
Figure 4-1 Flow chart of over all process of the Iris Extraction 52
Figure 4-2 Search point where likely to occur 53
Figure 4-3 Intensity sum over a) Horizontal and b) Vertical 54
Figure 4-4 The eight points selected 54
Figure 4 -5 Rectangular Search point 55
Figure 4-6 An example of an imperfect(left) & perfect (right) detection 56
Figure 4-7 - The searching region 56
Figure 4-8 Sum of intensity with different radius from the current center 58
Figure 4-9 Intensity change with different radius from the center 58
Figure 4-10 Five search points method 60
Figure 4-11 Case I, new position is found based on the valid matrix 61
Figure 4-12 Case II, when the new position can't be found using the valid matrix 62

Figure 4-13 The detected points of the parabola 63
Figure 5-14 Pupil is moved to the center of the iris 64
Figure 4-15 The iris and pupil boundaries are stretched to a standard size 65
Figure 4-16 Iris image after the rubbersheet process 65
Figure 4-17 How to mask off the bit 66
Figure 4-18 The mask 67
Figure 4-19 Masking two pictures by OR to get the result in the third picture 67
Figure 4-20 Gabor Function. 68
Figure 4-21 An illustration of the shifting process. 71
Figure 5-1 Inter-class Hamming distance distribution of the 'CASIA' 72
Figure 5-2 Histograph for same and for the different eyes (intra class) 73
Figure 5-3 General block diagram of improved Daugman's Algorithm 74

List of Tables

Table 2-1 Biometrics characteristics. 11
Table 2-2 Measurements for feature extraction. 19
Table 2-3 Thermographic image procedures 21
Table 2-4 Comparison of biometrics systems 33
Table 3-1 Probability of a False Match for Various HD Thresholds 47

1. Introduction

The first chapter gives an introductory topic. The second chapter is about my Major project overview and the background information on the general area of biometric science and image based biometrics in particular. This is extended by the third chapter which mainly explains theory that governs iris recognition. The fourth chapter is about implementation of the Iris Based Biometric System for Human Identification. Finally, in the fifth and sixth chapters results, discussions and conclusion have been given to examine the over all ideas and the last chapter points out areas of further continuation. The Matlab programming environment has been used as development tool. This reports referred to the M. Sc Thesis project on Iris Bases Biometrics System (IBBS) -for Human identification. There are three areas of interests namely: Biometrics, Iris recognition and human identification, which are explained in next paragraphs

Biometrics is automated methods of recognizing a person based on a physiological or behavioral characteristic [1][2]. A physiological characteristic is relatively stable physical characteristics, such as fingerprint, iris pattern, facial feature, hand silhouette, etc. This kind of measurement is basically unchanging and unalterable without significant duress. A behavioral characteristic is more a reflection of an individual's psychological makeup as signature, speech pattern, or how one types at a keyboard. The degree of intra-personal variation in a physical characteristic is smaller than a behavioral characteristic [3].

Iris recognition analyzes the features that exist in the colored tissue surrounding the pupil of eye which has more than 200 points that can be used for comparison, including rings, furrows and freckles. The scans use a regular video camera style and can be done from further away than a retinal scan. It will work through glasses fine and in fact has the ability to create an accurate enough measurement. The idea of using iris patterns for personal identification was originally proposed in 1936 by ophthalmologist Frank Burch. In 1987 two other ophthalmologists, Aran Safir and Leonard Flom, patented this idea, and in 1989 they asked John Daugman to try to create actual algorithms for iris recognition which is followed as main algorithm in this project. Well known and commercially available iris recognition system was pioneered by Daugman in 1993 [4].

A biometric system can be either an 'identification' system or a 'verification' (authentication) system. *Identification - One to Many*: Biometrics can be used to determine a person's identity even without his knowledge or consent. For example, scanning a crowd with a camera and using face recognition technology, one can determine matches against a known database. *Verification - One to One*: Biometrics can also be used to verify a person's identity. For example, one can grant physical access to a secure area in a building by using finger scans or can grant access to a bank account at an ATM by using retinal scan.

The main aim of this project is to reconstruct Daugman's algorithm on iris recognition based on grayscale NIR image. In addition, alternative solutions may be implemented to replace the original methods from Daugman's paper. The objective in using alternative solutions to the iris recognition system is to try to improve the iris recognition system. The whole iris recognition system is separated into hardware components and software components. The development of the software section of the iris recognition is the primary concerns for the project. The hardware component in this project is just a digital camera that is used to take in photo for use in the system.

The iris recognition can be separated into 4 stages: Input, Preprocessing, Encoding and Analysis. The input stage is the only stage that needs hardware equipment. In this stage an image is taken by a digital camera and the image is uploaded to the computer through USB port. This project concentrates on the development on the other stages. In those stages, iris pattern are encoded and then used to represent each individual person.

The major objectives of this project were to reconstruct Daugman's algorithm and improve the system after finishing the implementation on Daugman's algorithm.

2. Background and Project Overview

2.1 Introduction

As technology advances and information and intellectual properties are wanted by many unauthorized personnel. As a result, many organizations have being searching ways for more secure authentication methods for user access. Furthermore, security has always been an important concern to many people. From Immigration and Naturalization Service (INS) to banks, industrial, military systems, and personal are typical fields where security is highly valued. It is soon realized by many, that traditional security and identification are not sufficient enough; people need to find a new authentic system in the face of new technological reality [5].

Conventional security and identification systems are either knowledge based – like a social security number or a password, or token based – such as keys, ID cards. The conventional systems can be easily breached by others, ID cards and passwords can be lost, stolen or can be duplicated. In other words, it is not unique and not necessary represent the rightful user. Therefore, biometric systems are under intensive research for this particular reason.

2.2 What is Biometric?

Humans recognize each other according to their various characteristics for ages. People recognize others by their face when they meet and by their voice during conversation. These are part of biometric identification used naturally by people in their daily life. Biometrics is the development of statistical and mathematical methods applicable to data analysis problems in the biological sciences. The term "biometrics" is derived from the Greek words bio (life) and metric (to measure) simply “Biometrics” means “life-measurement”.

Biometrics relies on “something you are or you do”, on one of any number of unique characteristics that you can’t lose or forget. It is an identity verification of living, human individuals based on physiological and behavioral characteristics. In general, biometric system is not easily duplicated and unique to each individual. It is a step forwards from identify something you have and something you know, to something you are [6].

General biometric system: Biometrics uses physical characteristics, defined as the things we are and personal traits, it can consists of following [5],

Physical characteristics	Personal traits
chemical composition of body odor facial features and thermal emissions features of the eye - retina and iris fingerprints hand geometry skin pores wrist/hand veins	handwritten signature keystrokes or typing voiceprint

Table 2-1 Biometrics characteristics.

Same as many recognition systems, a general biometric system can consists of following sections, data collection, transmission, signal processing storage and decision [7], see Figure 2-1. It can considered that each section function independently, and errors can be introduced at each point in an additive way.

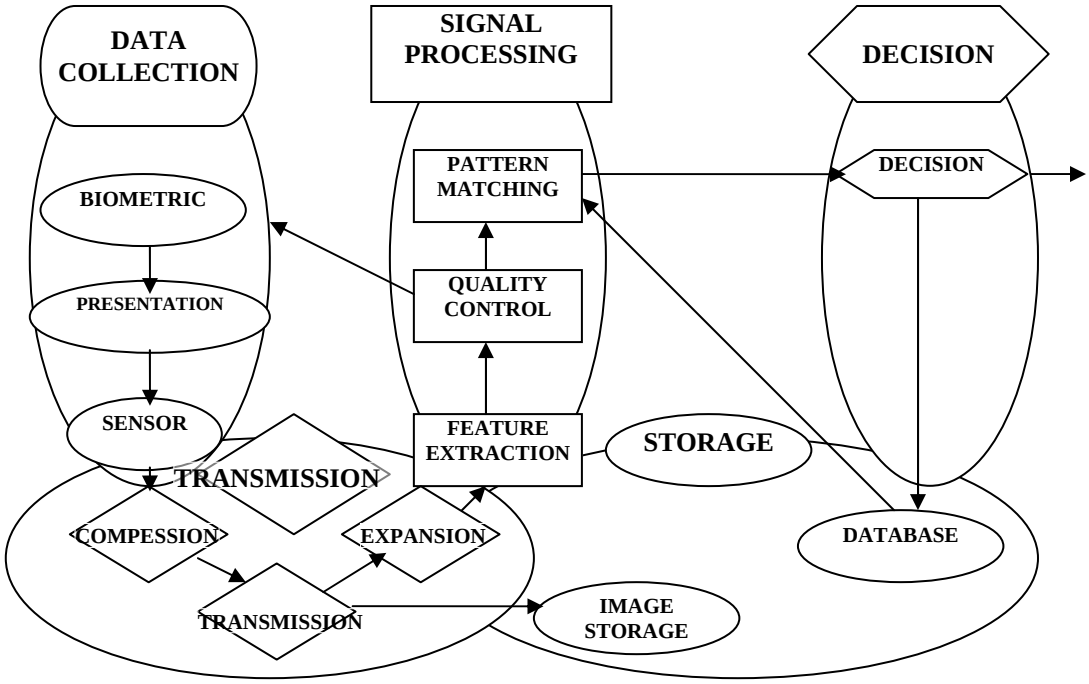

Figure 2-1. Generalized biometric system.

Data collection consists of sensors to obtain the raw biometric of the subject, and can output one or multidimensional signal. Usually, data are obtained in a normalized fashion, fingerprints are moderately pressed and rotation is minimized, faces are obtained in frontal or profiled view, etc. Data storage is usually separated from point of access, therefore the data have to be transmitted or distributed via a communication channel. Due to bandwidth, data compression may be required. The signal processing module takes the original biometric data and converts it into feature vectors. Depend on the applications, raw data might be stored as well as the obtained feature vectors. The decision subsystem compares the measured feature vectors with the storage data using the implemented system decision policy. If measures indicate a close relationship between the feature vector and compared template, a match is declared [7]. False matching and false non-matching error can occur, although for different systems error equation varied, a general equation can be developed [7][8]. Let M be the number of independent biometric measures the probability of false match FMRSR against any single record can be given by,

$$FMR_{SR} = \prod_{j=1}^{M} FMR_j(\tau_j) \tag{2.1}$$

Where $FMR_j(\tau_j)$ equal single comparison false match rate for the jth biometric and threshold τ. The probability for not making any false match in comparison in multiple records can be expressed as,

$$1 - FMR_{SYS} = (1 - FMR)^{PN} \tag{2.2}$$

Where FMR_{SYS} is the system false match rate, and N and P is number of records and percentage of the database to be searched respectively. For the single record false non-match rate,

$$1 - FNMR_{SR} = \prod_{j=1}^{M} [1 - FMR_j(\tau_j)] \tag{2.3}$$

More commonly used biometric system reliability indexes are FRR (False Reject Rate) which is the statistical probability that the system fails to recognize an enrolled person and FAR (False Accept Rate) which is the statistical probability that an imposter is recognized as an enrolled person. FRR and FAR are inversely dependent on each other and as within modern biometric systems identification:

$$\text{FRR } \varepsilon \text{ [0.0001\%, 0.1\%]} \tag{2.4}$$

$$\text{FAR } \varepsilon \text{ [0.0001\%, 5\%]} \tag{2.5}$$

They are very reliable, promising, universal and tampering resistant.

2.3 Image based biometric techniques

There are many biometric systems based on different characteristics and different part of the human body. However, people should look for the following in their biometrics systems [9],

- Universality - which means that each person should have the characteristic
- Uniqueness - which indicates that no two persons should be the same in terms of the characteristic
- Permanence - which means that the characteristic should not be changeable
- Collectability - which indicates that the characteristic can be measured quantitatively

From the above, various image based biometric techniques has been intensively studied. This thesis will discuss the following techniques, face, fingerprints, hand geometry, hand veins, iris, retina and signature.

2.3.1 Face

Face recognition technology (FRT) has applications in many wide ranges of fields, including commercial and law enforcement applications. This can be separate into two major categories. First is a static matching, example such as passport, credit cards, photo ID's, driver's licenses, etc. Second is real-time matching, such as surveillance video, airport control, etc. In the psychophysical and neuroscientific aspect, they have concerned on other research field which enlighten engineers to design algorithms and systems for machine recognition of human faces. A general face recognition problem can be, given still or video images of a scene to identify one or more persons in the scene using a stored database of faces [10]. With additional information such as race, age and gender can help to reduce the search. Recognition of the face is a relatively cheap and straightforward method. Identification based on acquiring a digital image on the target person and analyzing and extracting the facial characteristics for the comparison with the database.

Karhunen-Loeve (KL) expansion for the representation and recognition of faces is said to generate a lot of interest. The local descriptors are derived from regions that contain the eyes, mouth, nose, etc., using approaches such as deformable templates or eigen-expansion. Singular value decomposition (SVD) is described as deterministic counterpart of KL transform. After feature extraction, recognition is done, early approach such as feature point distance or nearest neighbor rule is used, and later

eigenpictures using eigenfaces and Euclidean distance approach is examined. Other methods using HyperBF network a neural network approach, dynamic link architecture, and Gabor wavelet decomposition methods are also discussed in [10].

A back-propagation neural network can be trained to recognize face images. However, a simple network can be very complex and difficult to train. A typical image recognition network requires N = m x n input neurons, one for each of the pixels in an m x n image. These are mapped to a number of hidden-layer neurons, p [11]. These in turn map to n output neurons, at least one of which is expected to fire on matching a particular face in the database. The hidden layer is considered to be a feature vector.

Eigenfaces is an application of principal component analysis (PCA) of an n-dimensional matrix. Start with a preprocessed image I(x,y), which can be considered as vector of dimension N2. An ensemble of images then maps to a collection of points in this huge space. The idea is to find a small set of faces (eigenfaces) that can approximately represent any point in the face space as a linear combination. Each of the eigenfaces is of dimension N x N, also can be interpreted as an image [11]. An image can be reduced to an eigenvector $\vec{B} = b_i$ which is the set of best-fit coefficients of an eigenface expansion. Eigenvector is then used to compare each of those in a database through distance matching, such as Cartesian distance.

Gabor wavelet is another widely used face recognition approach, it can be described by the (equation 2.6),

$$\psi_{\vec{k},\sigma}(\vec{x}) = \exp\left(-\frac{k^2 \mid \vec{x} \mid^2}{2\sigma^2}\right)\exp(i\vec{k}\vec{x}) \tag{2.6}$$

Where, k is the oscillating frequency of the wavelet, and the direction of the oscillation. σ is the rate at which the wavelet collapses to zero as one moves from its center outward. The main idea is to describe an arbitrary two-dimensional image function I(x,y) as a linear combination of a set of wavelets. The x, y plane is first subdivided into a grid of non-overlapping regions. At each grid point, the local image is decomposed into a set of wavelets chosen to represent a range of frequencies, directions and extents that "best" characterize that region [11]. By limiting k to a few values, the resulting coefficients become almost invariant to translation, scale and angle. The finite wavelet set at a particular point forms a feature vector called a jet, which characterize the image.

Also with elastically distorted grid, best match between two images can be obtained [11].

2.3.2 Fingerprints

One of the oldest biometric techniques is the fingerprint identification. Fingerprints were used as a means of positively identifying a person as an author of the document and are used in law enforcement. Fingerprint recognition has a lot of advantages, a fingerprint is compact, unique for every person, and stable over the lifetime. A predominate approach to fingerprint technique is the uses of minutiae [12], see Figure2-2.

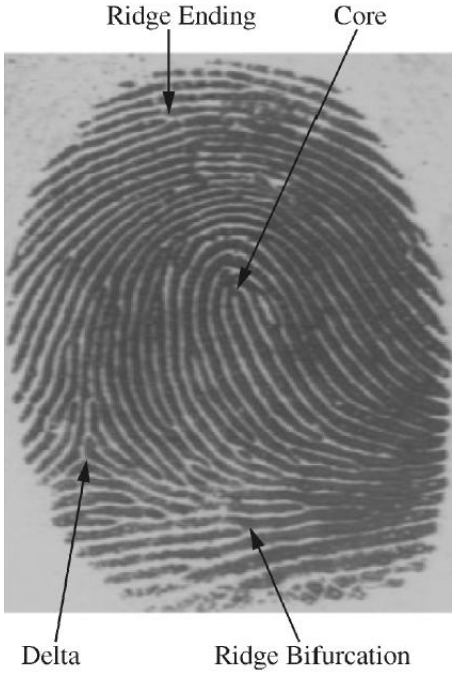

Figure 2-2. Minutiae, ridge endings and ridge bifurcations.

The traditional fingerprints are obtained by placing inked fingertip on paper; now compact solid state sensors are used. The solid state sensors can obtain patterns at 300 x 300 pixels at 500 dpi, and an optical sensor can have image size of 480 x 508 pixels at 500 dpi [13]. A typical algorithm for fingerprint feature extraction contains four stages, see in Figure 2-3.

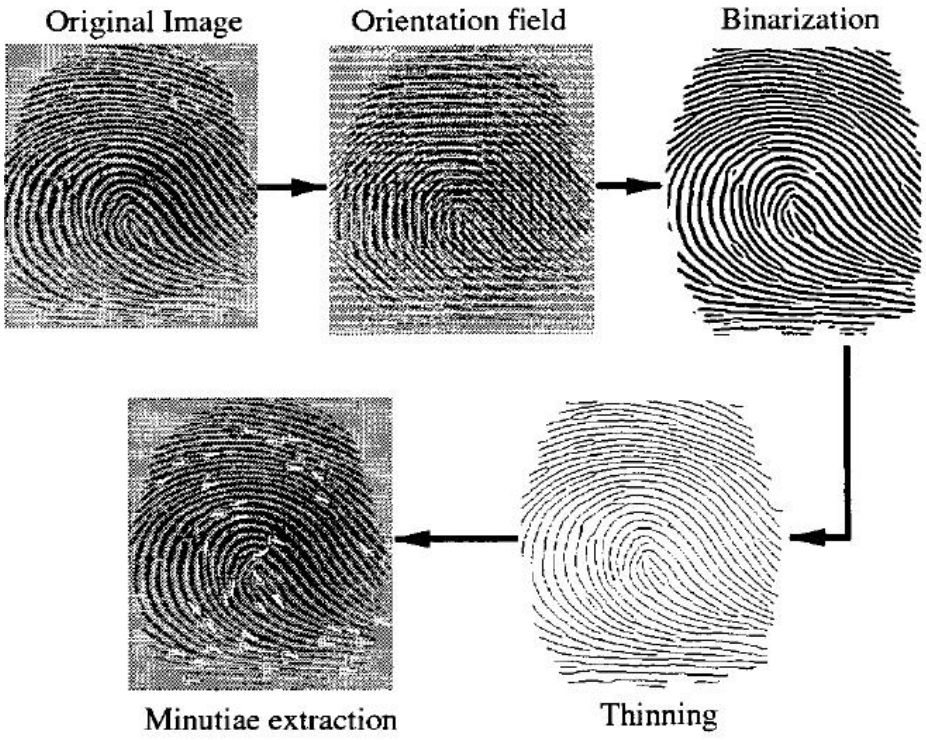

Figure 2-3. Typical fingerprint feature extraction algorithm.

The feature extraction first binarizes the ridges in a fingerprint image using masks that are capable of adaptively accentuating local maximum gray-level values along a direction normal to ridge direction [14]. Minutiae are determined as points that have one neighbor or more than two neighbors in skeletonized image [14].

Feature extraction approach differs between many papers, one simple minutiae extraction can be by applying the following filter, where resulting of 1 means ending, 2 a ridge, and 3 a bifurcation [12].

$$Minutiae\ Filter = \begin{bmatrix} 1 & 1 & 1 \\ 1 & 0 & 1 \\ 1 & 1 & 1 \end{bmatrix} \tag{2.7}$$

Or one might have the following filter [i], where R1 = R9

$$Minutiae\ Filter = \begin{array}{|c|c|c|} \hline R_1 & R_2 & R_3 \\ \hline R_8 & M & R_4 \\ \hline R_7 & R_6 & R_5 \\ \hline \end{array} \tag{2.8}$$

pixel M is a end point pixel M is a bifurcation

$$\sum_{k=1}^{8} \left| R(k+1) - R(k) \right| = 2 \tag{2.9}$$

$$\sum_{k=1}^{8} \left| R(k+1) - R(k) \right| = 6 \tag{2.10}$$

However more complicated feature extraction such as [13], [14] applied Gabor filters. [13] uses a bank of 8 Gabor filter with same frequency,0.1 pix-1, but different orientations (0° to 157.5° in steps of 22.5°). The frequency is chosen based on average inter-ridge distance in fingerprint, which is ~10 pixels. Therefore, there are 8 feature values for each cell in tessalation, and are concatenate to form 81 x 8 feature vector. In [14] the frequency is set to average ridge frequency (1/K), where K is the average inter-ridge distance. The Gabor filter parameters δx and δy are set to 4.0, and orientation is tuned to 0°. This is due to the extracted region is in the direction of minutiae. In general the result can be seen in Figure 2-4

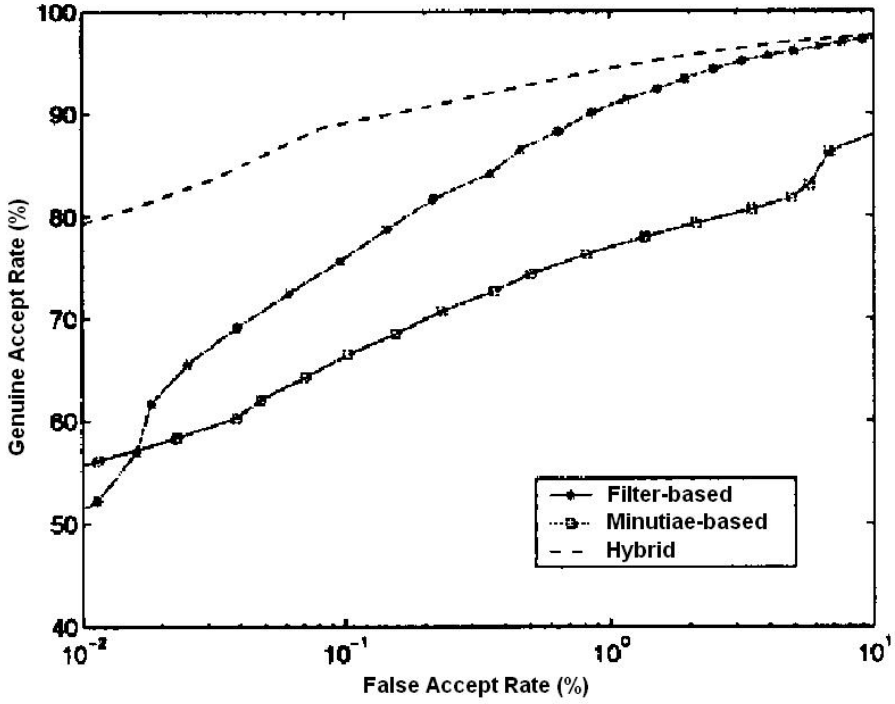

Figure 2-4 The ROC curve comparison.

Other enhancement algorithm such as preprocessing, mathematic algorithm and etc, have been discussed by [16], [17] and [18].

2.3.3 Hand geometry

Apart from face and fingerprints, hands are another major biometric of human being. Several hand parameters can be used for person identification,

1. hand shape and geometry
2. blood vessel patterns
3. palm line patterns

Hand geometry are consider to achieve medium level of security, it have several advantages [19].

1. Medium cost, only needs a platform and a low/medium resolution CCD camera.
2. It uses low-computational cost algorithms, which lead to fast results.
3. Low template size: from 9 to 25 bytes, this reduces the storage needs.
4. Very easy and attractive to users: leading to a nearly null user rejection.
5. Lack of relation to police, justice, and criminal records.

One of the prototype designs for this biometric system can be seen in Figure 2-5 ,

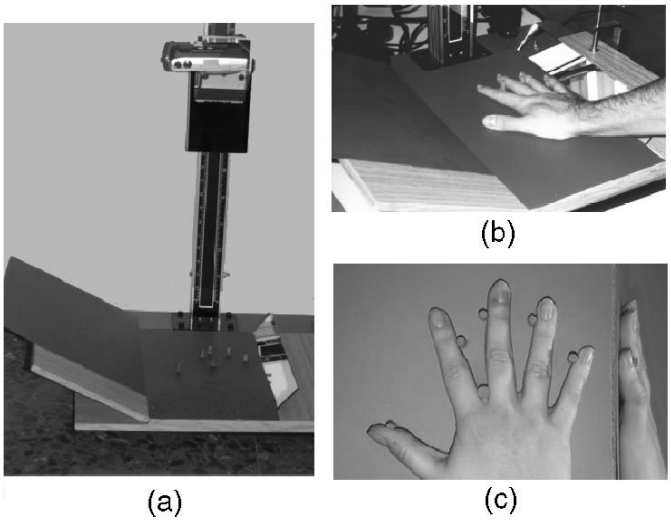

Figure 2-5 Prototype design
a) Platform and camera,
b)Placement of user's hand,
c) Photograph taken

The image obtained from the CCD camera is a 640 x 480 pixels color photograph in JPEG format [19]. Not only the view of the palm is taken, but also a lateral view is obtained with the side mirror. To extract features, the image is first convert into black and white, and spurious pixels are also removed at this point. Rotation and resizing of image are also done to eliminate variations caused by position of camera. This is follow by Sobel edge detection to extract contours of the hand [19]. The measurements for feature extractions consists of following [19], refer to Figure2-6,

Widths	Each of the four fingers is measured in different heights, avoiding the pressure points (w11-w44). The width of the palm (w0) is also measured and the interfinger distance at point P1, P2 and P3, vertical and horizontal coordinates.
Heights	The middle finger, the little finger, and the palm (h1, h2, h3).
Deviations	The distance between a middle point of the finger and the straight line, $$deviation = P_{12}^{x} - \left(\frac{P_{14}^{x} - P_{1}^{x}}{P_{14}^{y} - P_{1}^{y}} \right) (P_{12}^{y} - P_{1}^{y}) \quad (2.10)$$
Angles	Between interfinger point and horizontal.

Table 2-2 Measurements for feature extraction.

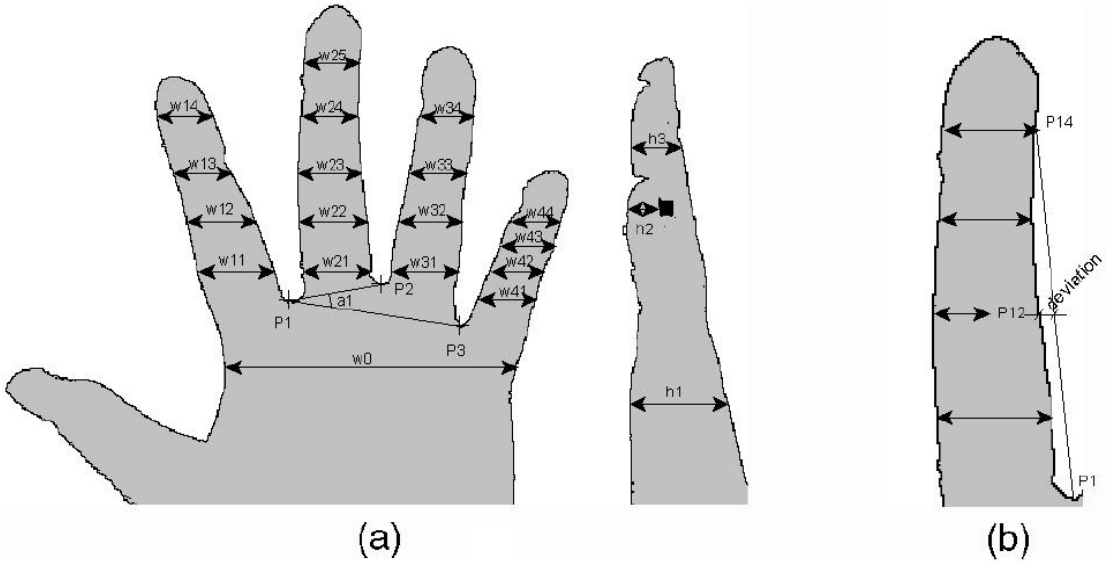

Figure 2-6. a) Location of measurement point for feature extraction, b) details of the deviation measurement.

In total 31 features are extracted, several classifier algorithm have been discussed in [19]. These are, Euclidean distance, Hamming distance, Gaussian mixture models (GMMs), and Radial basis function neural networks (RBF). The Euclidean distance performs using the following equation,

$$d = \sqrt{\sum_{i=1}^{L} (x_i - t_i)^2} \quad (2.11)$$

where L is the dimension of the feature vector, xi is the i^{th} component of the sample feature vector, and t_i is the i^{th} component of the template feature vector. Hamming distance measure the difference between numbers of components that differ in value.

Assume that feature follow a Gaussian distribution, both mean and standard deviation of the samples are obtained, size of the template increase from 25 to 50 bytes.

$$d(x_i, t_i^m) = \#\left\{i \in \{1,\ldots,L\} / \left|x_i - t_i^m\right| > t_i^v\right\} \tag{2.12}$$

where t_i^m is the mean for the i^{th} component, and t_i^v the factor of the standard deviation for the i^{th} component. GMMs technique uses an approach between statistical methods and the neural networks [19]. The probability density of a sample belonging to a class u is,

$$p(\vec{x}/u) = \sum_{i=1}^{M} \frac{c_i}{(2\pi)^{L/2}\left|\sum_i\right|^{1/2}} \exp\left\{-\frac{1}{2}(\vec{x}-\vec{u}_i)^T \sum_i^{-1} (\vec{x}-\vec{u}_i)\right\} \tag{2.13}$$

c_i being the weights of each of the Gaussian models, u_i the mean vector of each model, $\sum i$ the covariance matrix of each model, M the number of models, and L the dimension of feature vectors. RBF consists of two layers, one is base on a radial basis function, such as Gaussian distribution the send is a linear layer.

It is found from [19], that GMM give the best result is both classification (about 96 percent success) and verification with a higher computational cost and template size [19], [20]. Performance improves with increasing enrollment size, except Euclidean distance and RBFs. The Equal Error Rate (FAR = FRR), remains similar in each technique for the different feature vector sizes.

2.3.4 Hand veins

Not like fingerprint, hand shape and iris/retina biometric systems, hand veins have advantages over contamination issues and will not pose discomfort to the user [21]. The process algorithm consists of image acquisition unit, processing units and recognition module [21], [22]. Under the visible light, vein structure is not always easily seen; it depends on factors such as age, levels of subcutaneous fat, ambient temperature and humidity, physical activity and hand positions, not to mention hairs and scars. [21] proposed using conventional CCD fitted with IR cold source for imaging acquisition. IR emits wavelength of 880 nm ± 25 nm, provide better contrast than ordinary tungsten filament bulbs. Preferably a IR filter is inserted to eliminate any visible light reaches CCD sensor [21]. Below shows a proposed hand vein acquisition device, see Figure2-7.

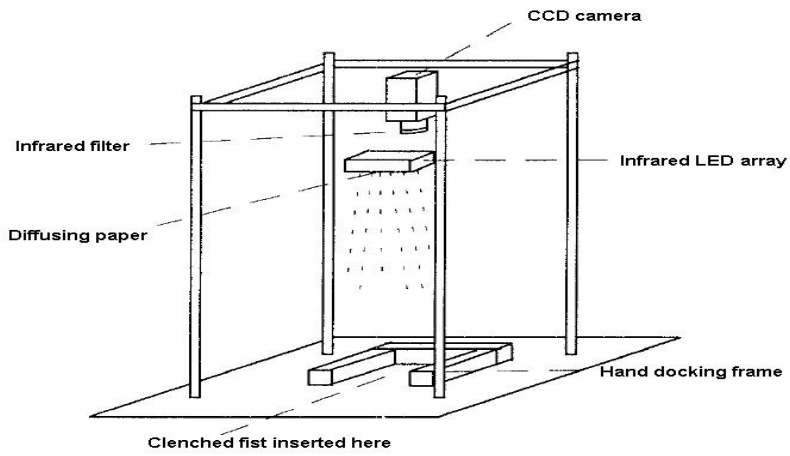

Figure 2-7. Schematic of imaging unit.

The segmentation of the vein pattern consists of procedure several numbers of processes,

Attenuate impulse noise and enhance contrast	Moving average is applied
Determine the domain of the hand	Morphological gradient is used to separate background
Reduce the domain	Morphological openings, closings and erosion are applied
Remove hair, shin pores and other noise	Max and min of independent opening and closing using linear structuring elements are applied
Normalize the background	Brightness surface is subtracted, leaving only the vein structure and background
Threshold out the vein pattern	Morphological gradient is applied to obtain a threshold value that separates the vein and background
Remove artifacts, fill holes	Binary alternating sequential filter, is used to remove threshold artifacts and fill holes in vein structure
Thin the patter down to its medial axis	Modified Zhang and Suen algorithm is used
Prune the medial axis	Automatic pruning algorithm is used

Table 2-3. Thermographic image procedures

It is noted that significant horizontal positional noise during docking for different registration process [21]. The proposed matching approach compares medial axis and coding algorithm, constrained sequential correlation. It is a variation on the traditional correlation methods used for template matching. The reference or library signature is first dilated by a hexagonal structuring element. The test signature is then superimposed on this reference buffer and the percentage of pixels contained within the buffer determined. Due to horizontal translation error, test signature is sequentially translated horizontally and compared against the reference buffer [21]. The horizontal translation is limit to ± 30 pixels. The highest match percentage is said to be the forward similarity, where reverse similarity is obtained by dilate the test signature and reference signature is sequentially correlated until the maximum measure is obtained. By setting the forward and reverse minimum percentage to 75% and 60% respectively, the resultant FRR is 7.5% and FAR is 0%. If forward percentage is lowered to 70%, FRR improved down to 5% and FAR remains the same [21].

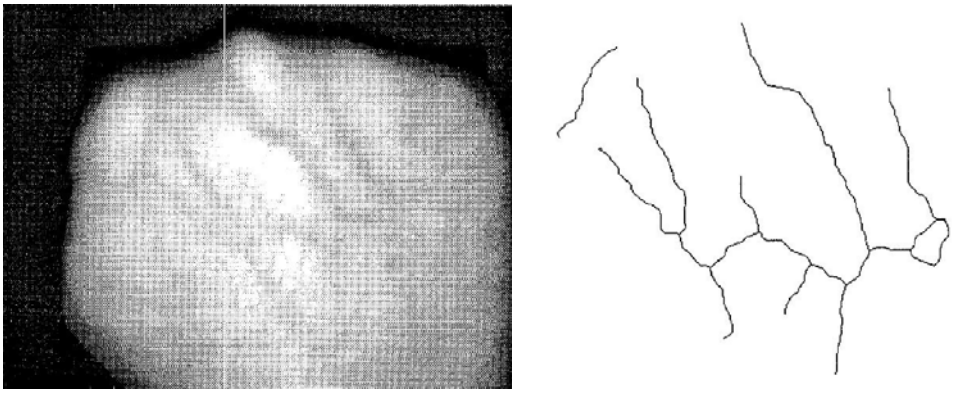

Figure 2-8. Left is original captured image, right is vein structure after prune the medial axis

Conventional method uses low pass filter follow by high pass filter, after that threshold is applied with bilinear interpolation and modified median filter to obtain hand vein in region of interest (ROI) [22]. The Gaussian low pass filter is a 3 x 3 spatial filter with equation,

$$Z(5) = \sum_{i=1}^{9} W(i)Z(i) \tag{2.14}$$

$$Filtered\ image = \begin{array}{|c|c|c|} \hline Z_1 & Z_2 & Z_3 \\ \hline Z_4 & Z_5 & Z_6 \\ \hline Z_7 & Z_8 & Z_9 \\ \hline \end{array} \times \begin{array}{|c|c|c|} \hline W_1 & W_2 & W_3 \\ \hline W_4 & W_5 & W_6 \\ \hline W_7 & W_8 & W_9 \\ \hline \end{array} \tag{2.5}$$

Due to heavy computation load [22] introduce a way of enhancing the algorithm. Both the coefficients for the Gaussian low pass filter and the low pass filter are designed to

have 7-tap CSD (canonical signed digit) codes at the maximum. Also, for the normalization, the decimation method is used. It is said that, CSD code is an effective code for designing a FIR filter without a multiplier. The proposed preprocessing algorithm follows the same steps as the conventional method, except that the coefficients for each filter are made of CSD codes. The general CSD code is equal to,

$$W_j = \sum_{i=1}^{M_j} S_i 2^{-i} \tag{2.16}$$

where j = 1, 2, …, 121, Si∈{-1, 0, 1} and M is an integer. Instead a 3 x 3 Gaussian low pass filter, a 11 x 11 spatial filter is applied instead. Is it found that Gaussian filter is 94.88% reliable relative to their experiment, and maximum of 0.001% FAR can be obtained by varying the threshold level [22].

2.3.5 Iris

Another biometric non-invasive system is the use of color ring around the pupil on the surface of the eye. Iris contains unique texture and is complex enough to be used as a biometric signature. Compared with other biometric features such as face and fingerprint, iris patterns are more stable and reliable. It is unique to people and stable with age [23]. Figure 2-9, shows a typical example of an iris and extracted texture image.

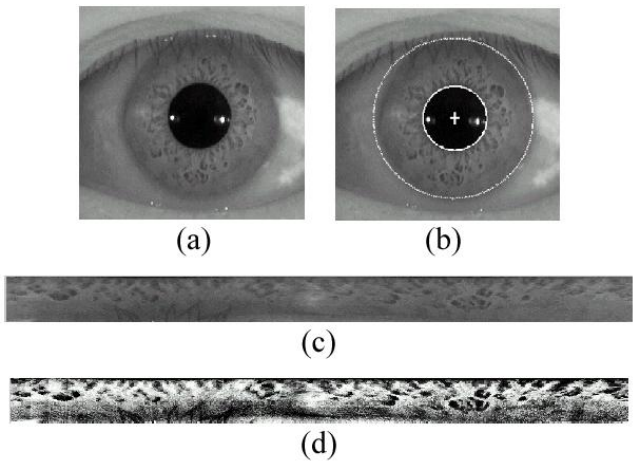

Figure 2-9. (a) Iris image (b) iris localization (c) unwrapped texture image (d) texture image after enhancement

Iris is highly randomized and its suitability as an exceptionally accurate biometric derives from its [24],

- extremely data-rich physical structure
- genetic independence, no two eyes are the same
- stability over time
- physical protection by a transparent window (the cornea) that does not inhibit external view ability

There are wide range of extraction and encoding methods, such as, Daugman Method, multi-channel Gabor filtering, Dyadic wavelet transfmor [25], etc. Also, iris code is calculated using circular bands that have been adjusted to conform to the iris and pupil boundaries. Daugman is the first method to describe the extraction and encoding process [26]. The system contains eight circular bands and generates 512-byte iris code, see Figure 2-10 [24].

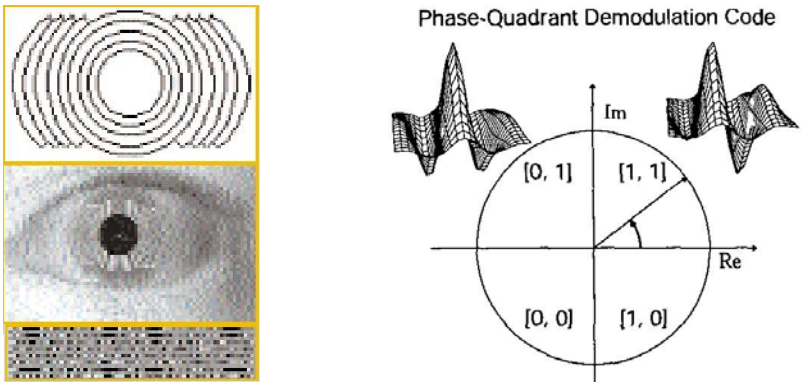

a) b)

Figure 2-10. a) Daugman system, top 8 circular band, bottom iris code b) demodulation code

After boundaries have been located, any occluding eyelids detected, and reflections or eyelashes excluded, the isolated iris is mapped to size-invariant coordinates and demodulated to extract its phase information using quadrature 2D Gabor wavelets [26]. A given area of the iris is projected onto complex-valued 2D Gabor wavelet using,

$$h_{\{\mathrm{Re,Im}\}} = \mathrm{sgn}_{\{\mathrm{Re,Im}\}} \int_{\rho}\int_{\phi} I(\rho,\phi) e^{-iw(\theta_0-\phi)} e^{-(r_0-\rho)^2/\alpha^2} e^{-(\theta_0-\phi)^2/\beta^2} \rho \, d\rho \, d\phi \tag{2.17}$$

where h{Re,Im} can be regarded as a complex-valued bit whose real and imaginary parts are either 1 or 0 (sgn) depending on the sign of the 2D integral. I(ρ,ϕ) is the raw iris image in a dimensionless polar coordinate system that is size- and translation-

invariant, and which also corrects for pupil dilation. α and β are the multi-scale 2D wavelet size parameters, spanning a 8-fold range from 0.15mm to 1.2mm on the iris, and w is wavelet frequency spanning 3 octaves in inverse proportion to β. (r0,θ0) represent the polar coordinates of each region of iris for which the phasor coordinates h{Re,Im} are computed [26]. 2,048 such phase bits (256 bytes) are computed for each iris and equal amount of masking bits are computed to signify any region is obscured by eyelids, eyelash, specular reflections, boundary artifacts or poor signal-to-noise ratio. Hamming distance is used to measure the similarity between any two irises, whose two phase code bit vectors are denoted {codeA, codeB} and mask bit vectors are {maskA, maskB} with Boolean operation [26],

$$HD = \frac{\left\| (codeA \otimes codeB) \cap maskA \cap maskB \right\|}{\left\| maskA \cap maskB \right\|} \tag{2.18}$$

For two identical iris codes, the HD is zero; for two perfectly unmatched iris codes, the HD is 1. For different irises, the average HD is about 0.5 [26]. The observed mean HD was p = 0.499 with standard deviation σ = 0. 317, which is close fit to theoretical values [26]. Generally, an HD threshold of 0.32 can reliably differentiate authentic users from impostors [26].

An alternative approach to this iris system can be the use of multi-channel Gabor filtering and wavelet transform [26]. The boundaries can be taken by two circles, usually not co-centric. Compared with the other part of the eye, the pupil is much darker, therefore, inner boundary between the pupil and the iris is determined by means of thresholding. The outer boundary is determined by maximizing changes of the perimeter-normalized sum of gray level values along the circle [26].

Due to size of pupil can be varied, it is normalized to a rectangular block of a fixed size. Local histogram equalization is also performed to reduce the effect of non-uniform illumination, see Figure2-9. The multi-channel Gabor filtering technique involves of cortical channels, each cortical channel is modeled by a pair of Gabor filters opposite symmetry to each other.

$$h_e(x,y) = g(x,y) \cdot \cos[2\pi f(x\cos\theta + y\sin\theta)]$$
$$h_o(x,y) = g(x,y) \cdot \sin[2\pi f(x\cos\theta + y\sin\theta)] \tag{2.19.a and 2.19.b}$$

where g(x,y) is a 2D Guassian function, f and θ are the central frequency and orientation. The central frequencies used in [26] are 2, 4, 8, 16, 32 and 64 cycles/degree. For each central frequency f, filtering is performed at θ = 0°, 45°, 90° and 135°. Which produces 24 output images (4 for each frequency), from which the iris features are extracted. These features are the mean and the standard deviation of each output image. Therefore, 48 features per input image are calculated, and all 48 features are used for testing.

A 2D wavelet transform can be treated as two separate 1-D wavelet transforms [23]. A set of sub-images at different resolution level are obtained after applying wavelet transform. The mean and variance of each wavelet sub-image are extracted as texture features. Only five low resolution levels, excluding the coarsest level, are used. This makes the 26 extracted features robust in a noisy environment [23]. Weighted Euclidean Distance is used as classifier,

$$WED(k) = \sum_{i=1}^{N} \frac{(f_i - f_i^{(k)})^2}{(\delta_i^{(k)})^2} \tag{2.20}$$

where fi denotes the ith feature of the unknown iris, $f_i(k)$ and $\delta_i(k)$ denots the i^{th} feature and its standard deviation of iris k, N is the total number of features extracted from a single iris. It is found that, a classification rate of 93.8% was obtained when either all the 48 features were used or features at f = 2, 4, 8, 16, 32 were used. And the wavelet transform can obtained an accuracy of 82.5% [26]. Other methods such as Circular Symmetric Filters [27] can obtain correct classification rate of 93.2% to 99.85%.

2.3.6 Retina

A retina-based biometric involves analyzing the pattern of blood vessels captured by using a low-intensity light source through an optical coupler to scan the unique patterns in the back of the eye [28]. Retina is not directly visible and so a coherent infrared light source is necessary to illuminate the retina. The infrared energy is absorbed faster by blood vessels in the retina than by the surrounding tissue. Retinal scanning can be quite accurate but does require the user to look into a receptacle and focus on a given point. However it is not convenient if wearing glasses or if one concerned about a close contact with the reading device [28].

A most important drawback of the retina scan is its intrusiveness. The light source must be directed through the cornea of the eye, and operation of the retina scanner is not easy. However, in healthy individuals, the vascular pattern in the retina does not change over the course of an individual's life [29]. Although retina scan is more susceptible to some diseases than the iris scan, but such diseases are relatively rare. Due to its inherent properties of not user-friendly and expansive, it is rarely used today. A typical retinal scanned image is shown in Figure2-11.

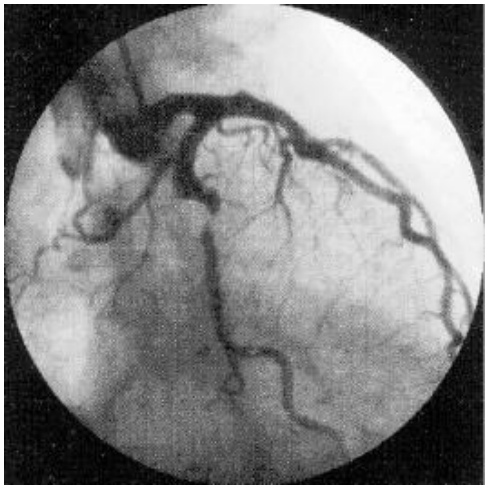

Figure 12-11 Retinal scanned image

Paper [29] propose a general framework of adaptive local thresholding using a verification-based multithreshold probing scheme. It is assumed that, given a binary image BT resulting from some threshold T, decision can be made if any region in BT can be accepted as an object by means of a classification procedure. A pixel with intensity lower than or equal to T is marked as a vessel candidate and all other pixels as background. Vessels are considered to be curvilinear structures in BT, i.e., lines or curves with some limited width [29]. The approach to vessel detection in BT consists of three steps: 1) perform an Euclidean distance transform on BT to obtain a distance map, 2) prune the vessel candidates by distance map retain only center line pixels of curvilinear bands, 3) reconstruct the curvilinear bands from their center line pixels. The reconstructed curvilinear bands give that part of the vessel network that is made visible by the particular threshold T [29].

Fast algorithm for Euclidean distance transform is applied. For each candidate vessel point, the resulting distance map contains the distance to its nearest background pixel and the position of that background pixel [29]. The pruning operation uses two

measures, ϕ and d, to quantify the likelihood of a vessel candidate being a center line pixel of a curvilinear band of limited width, see Figure2-12

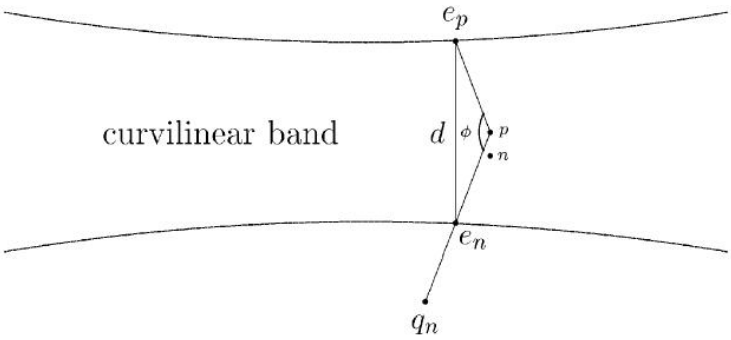

Figure 2-12. Quantities for testing curvilinear bands.

where p and n represent a vessel candidate and one of the eight neighbors from its neighborhood Np, respectively, ep and en are their corresponding nearest background pixel. The two measures are defined by,

$$\phi = \max_{n \in N_p} angle(\overline{pe}_p, \overline{pe}_n) = \max_{n \in N_p} \frac{180}{\pi} \cdot \arccos \frac{\overline{pe}_p \cdot \overline{pe}_n}{\left\|\overline{pe}_p\right\| \cdot \left\|\overline{pe}_n\right\|} \tag{2.21}$$

$$d = \max_{n \in N_p} \left\|\overline{e}_p \overline{e}_n\right\| \tag{2.22}$$

The overall improvement result can be seen in Figure 2-13 below,

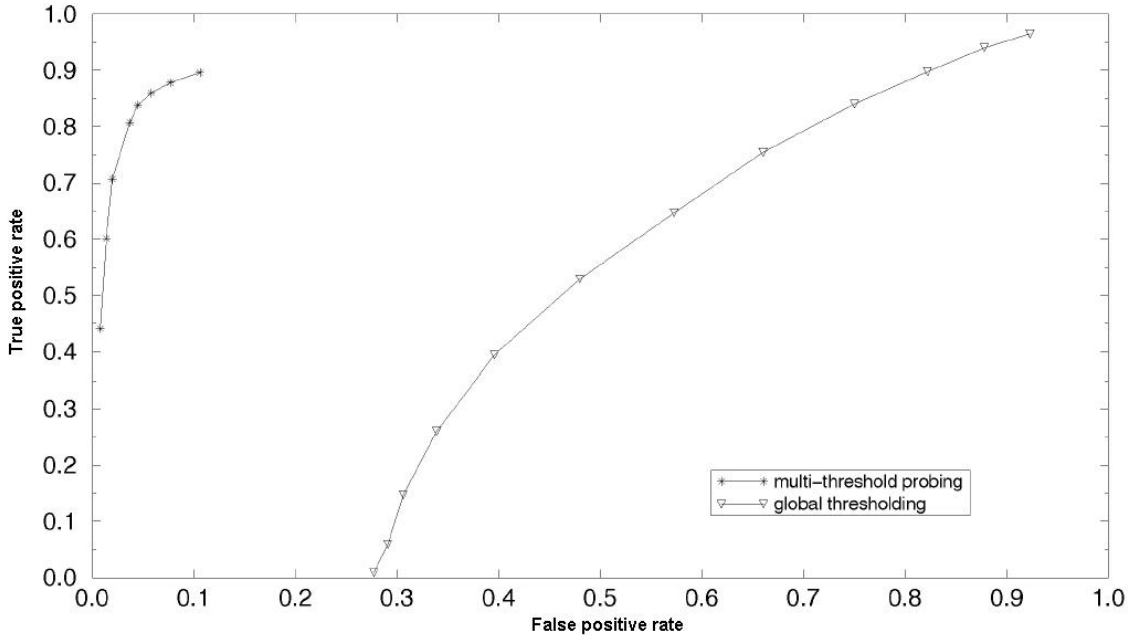

Figure 2-13. Proposed approach versus global thresholding.

2.3.7 Signature

Signature differ from above mentioned biometric system, it is a trait that characterize single individual. Signature verification analyzes the way a user signs his or her name.

This biometric system can be put into two categories, on-line and off-line methods. On-line methods take consideration of signing features such as speed, velocity, rhythm and pressure are as important as the finished signature's static shape [30]. Where as, off-line classification methods are having signature signed on a sheet and scanned. People are used to signatures as a means of transaction-related identity verification, and most would see nothing unusual in extending this to encompass biometrics. Signature verification devices are reasonably accurate in operation and obviously lend themselves to applications where a signature is an accepted identifier [30]. Various kinds of devices are used to capture the signature dynamics, such as the traditional tablets or special purpose devices. Special pens are able to capture movements in all 3 dimensions. Tablets are used to capture 2D coordinates and the pressure, but it has two significant disadvantages. Usually the resulting digitalized signature looks different from the usual user signature, and sometimes while signing the user does not see what has been written so far. This is a considerable drawback for many (unexperienced) users.

A proposed off-line classification method to compensate the less information is raised by [30]. The proposed method utilizes Hidden Markov Models (HMM) as the classifiers. Before, HMM is applied, scanned signature image have to go through the following,

1. Noise filtering, to remove the noise including noise added by scan process.
2. Correcting the inclination of the sheet in the scanner.
3. Binarization of the graphic.
4. Center the signature image.
5. Skeletonization or thinning algorithm.

Feature extraction is then performed; first try to obtain the starting point (more on the left and more below). Then code the direction using the direction matrix, see Figure 2-14, the obtained direction vector indicates the direction of the next pixel signature. When come to a crossing point, the straight direction is followed and this point is returned after the straight direction line is fished. The direction vector usually have 300 elements [30].

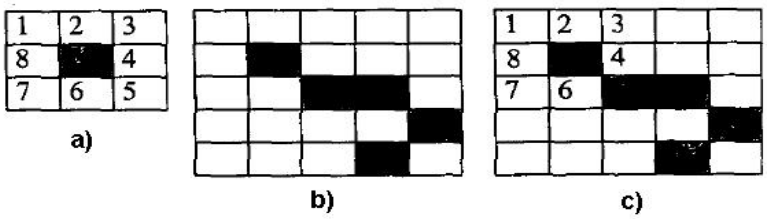

Figure 2-14. a) Directional matrix b) Signature c) Apply matrix to obtain direction vector = [5 4 5 7]

In recognition stage of an input or signature vector sequence X, each HMM model λ_i, i = {1,2,…,M}, with M equal to the number of different signatures, estimates the "a posteriori" probabilities P(X | λi), and the input sequence X is assigned to the j signature which provides the maximum score (maxnet),

$$X \in \lambda_i \quad if \ \ j = \arg\max_{i=1,2,\ldots,M} P(X \mid \lambda_i) \tag{2.23}$$

The resultant system decrease greatly when the number of signature increases. The recognition and verification rates are for 30 signatures are 76.6% and 92% respectively.

On-line verification signature verification methods can be further divided into two groups: direct methods (using the raw functions of time) and indirect methods (using parameters) [31]. With direct methods, the signature is stored as a discrete function to be compared to a standard from the same writer, previously computed during an enrolment stage. Such methods simplify data acquisition but comparison can become a hard task. For indirect methods, it requires a lot of effort preparing data to be processed, but the comparison is quite simple and efficient [31]. One direct method system, mentioned in [31], relies on three pseudo-distance measures (shape, motion and writing pressure) derived from coordinate and writing pressure functions through the application of a technique known as Dynamic Time Warping (DTW). It is reported to have over 90% success rate. Another approach is the use of Fast Fourier Transform as an alternative to time warping. It is suggested that working in the frequency domain would eliminate the need to worry about temporal misalignments between the functions to be compared. It is concluded that the FFT can be useful as a method for the selection of features for signature verification [31].

Alternative approach could be wavelet base method, where the signature to be tested is collected from an electronic pad as two functions in time (x(t),y(t)). It is numerically processed to generate numbers that represent the distance between it and a reference signature (standard), computed in a previous enrolment stage. The numerical treatment includes resampling to a uniform mesh, correction of elementary distortions between

curves (such as spurious displacements and rotations), applying wavelet transforms to produce features and finally nonlinear comparison in time (Dynamic Time Warping).

The decomposition of the functions x(t) and y(t) with wavelet transform generates approximations and details like those showed in Figure Figure 2-15 to an original example of x(t) [31].

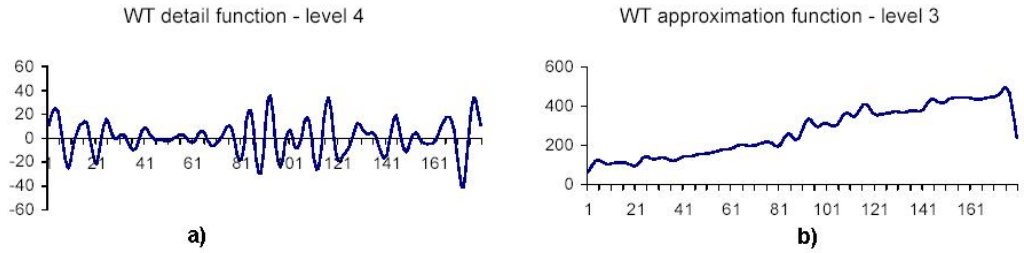

Figure 2-15 Function x(t) after wavelet transform.

Each zero-crossing of the detail curve at the 4th level of resolution (this level was chosen empirically, by trial and error), three parameters are extracted: its abscissa, the integral between consecutive zero-crossings,

$$vi_k = \int_{ZC_{k-1}}^{ZC_k} WD4(t)dt \tag{2.24}$$

and the corresponding amplitude to the same abscissa in the approximation function at 3rd level,

$$va_k = WA3(zc_k) \tag{2.25}$$

As it has been demonstrated that this information suffices to a complete reconstruction of the nontransformed curve [31]. Before measuring distance, it is necessary to identify a suitable correspondence between zerocrossings, which is accomplished with the Dynamic Time Warping (DTW) algorithm. It consists of a linear programming technique, in which the time axis of the reference curve is fixed, while the time axis of the test curve is nonlinearly adjusted, so as to minimize the norm of the global distance between the curves[31]. It is found that the Dynamic Time Warping algorithm on features extracted with the application of wavelet transforms, is suitable to on-line signature verification. Furthermore, it is only with the inclusion of wavelet transform that proposed system can prevent trained forgeries to be accepted (0% FAR).

2.4 Multiple biometric

In practice, a biometric characteristic that satisfies the requirements mentioned in section image based biometric techniques may not always be feasible for a practical biometric system. In a practical biometric system, there are a number of other issues which should be considered, including [32],

1. Performance, which refers to the achievable identification accuracy, speed, robustness, the resource requirements to achieve the desired identification accuracy and speed, as well as operational or environmental factors that affect the identification accuracy and speed.
2. Acceptability, which indicates the extent to which people are willing to accept a particular biometrics in their daily life.
3. Circumvention, which reflects how easy it is to fool the system by fraudulent methods.

Also, single biometric system has some limitations, such as noisy data, limited degrees of freedom [33]. In searching for a better more reliable and cheaper solution, fusion techniques have been examined by many researches, which also known as multi-modal biometrics. This can address the problem of non-universality due to wider coverage, and provide anti-spoofing measures by making it difficult for intruder to "steal" multiple biometric traits [33]. Commonly used classifier combination schemes such as the product rule, sum rule, min rule, max rule, media rule and the majority rule were derived from a common theoretical framework under different assumptions by using different approximations [34]. In [33] it is discussed that different threshold or weights can be given to different user, to reduce the importance of less reliable biometric traits. It is found by doing this, FRR can be improved. As well it can reduce the failure to enroll problem by assigning smaller weights to those noisy biometrics. Also, in [32], the proposed integration of face and fingerprints overcomes the limitations of both face-recognition systems and fingerprint-verification systems. The decision-fusion scheme formulated in the system enables performance improvement by integrating multiple cues with different confidence measures, with FRR of 9.8% and FAR of 0.001%. Other fusion techniques have been mentioned in [34], these are Bayes theory, clustering algorithms such as fuzzy K-means, fuzzy vector quantization and median radial basis function. Also vector machines using polynomial kernels and Bayesian classifiers (also used by [35] for multisensor fusion) are said to outperform Fisher's linear discriminant [34]. Not only fusion between biometric, fusions within a same biometric systems using

different expert can also improve the overall performance, such as the fusion of multiple experts in face recognition [36]and [37].

Depend on application different biometric systems will be more suited than others. It is known that there is no one best biometric technology, where different applications require different biometrics. Some will be more reliable in exchange for cost and vise versa, see Figure 2-16 [38]

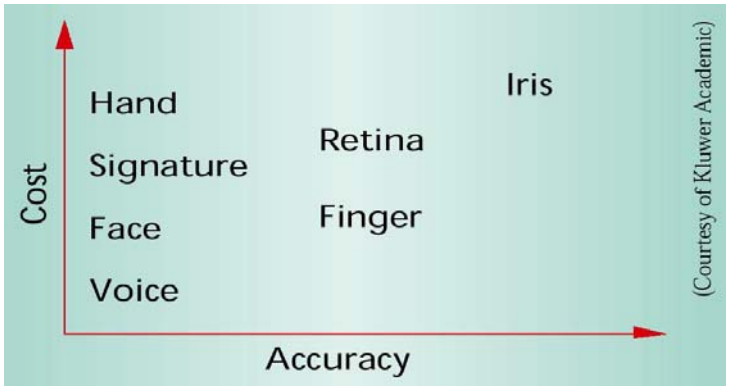

Figure 2-16 Cost vs accuracy

Proper design and implementation of the biometric system can indeed increase the overall security. Furthermore, multiple biometric fusions can be done to obtain a relative cheaper reliable solution. The imaged base biometric utilize many similar functions such as Gabor filters and wavelet transforms. Image based can be combined with other biometrics to give more realible results such as liveliness (ECG biometric) or thermal imaging or Gait based biometric systems. A summary of comparison of biometrics is shown in table below Table 2-4,

	Ease of use	**Error incidence**	**Accuracy**	**User acceptance**	**Required security level**	**Long-term stability**
Fingerprint	High	Dryness, dirt	High	Medium	High	High
Hand Geometry	High	Hand injury, age	High	Medium	Medium	Medium
Iris	Medium	Poor Lighting	Very High	Medium	Very High	High
Retina	Low	Glasses	Very High	Medium	High	High
Signature	High	Changing signatures	High	Very high	Medium	Medium
Face	Medium	Lighting, age, hair, glasses	High	Medium	Medium	Medium

Table 2-4. Comparison of biometrics systems

2.5 Iris Recognition

This project concentrates on one of the available biometrics feature which is, Iris-scan also called Iris Recognition. The iris recognition system is a biometric technology that takes the iris pattern of the human eyes as the physical features to identify and verify the access level of a person. The input device of this system is usually a digital camera that takes images of the user's iris. After that, any array of data is extracted from the image and converted into 256 bytes for the system to verify [4].

The unique characteristic of the iris makes it available to be used in the biometrics system [4][39][40]. The iris pattern remains unchanged throughout the lifetime of a human [4][39][40]. The formation of the iris pattern is independent of generic factors. As a result of that, the iris pattern is unique [4][39][40]. Even with the left and right eyes of the same person, the iris patterns for them are totally different and twins do not have identical iris pattern as well [4][39][40]. This makes iris recognition better than most of the other biometrics recognition systems. There is a very low probability that two people have the same iris pattern because of the properties listed above [41][42]. Therefore, the iris pattern can be used in biometrics identification system and it is a good solution for the security problem that the human society is facing now.

The advantages of using iris recognition system are :

- Iris is an internal organ and it is protected by the eye lid
- No physical contact is needed to get the iris pattern
- Iris patterns are very random
- Can detect if the eye is natural and alive by taking multiple images
- Infant identification
- Iris patterns are not strongly influenced by genetics
- Iris patterns have a good performance over time, i.e. stable
- Fast processing time
- 256-1024 bytes iris code is needed for each individual

However, there are some disadvantages :

- Iris is small, therefore it is hard to detect from a distance
- The detection of iris is difficult when the target is moving. This is because it
- is dependent on the head movement, eye movement and the pupil
- The cornea layer is curved, wet and there are some reflections. These cause distortion to the image
- Eyelashes, corrective lens and reflections may blur iris pattern
- Iris will deform when the pupil changes its size.
- High Cost

2.6 Project Overview

The main aim of the project is to reconstruct an iris recognition based on Daugman's algorithm on iris recognition. This is because Daugman is the first person to publish the algorithm on iris recognition and most commercial iris recognition systems are implemented using his algorithm. After finish reconstructing his algorithm, various testing will be done. Individual sections will be improved by using different algorithms.

The security demands are increasing nowadays and finding useful trustful algorithms to prevent/identify unsolicited visitors is very important. Iris Recognition is one of those methods. It based on the fact that every eye has a unique characteristics (in its Iris) which separate the person from other people, and even separating his right eye from his left eye. The project was divided into 2 areas:

Part I. Image Processing - isolating the iris:
Part II Signal Processing - characterizing it as a matrix unique to every person.

2.7 Programming Language

A program is needed to process the iris code and act as the Graphical interface with the user. The program needs to be efficient in terms of processing and user friendliness to the user. As a result of that, programming language with a good support on image processing and fast execution time is needed. There is a wide range of programming

languages that can be used to write the program of the iris recognition system, such a Python, Java, Matlab and C++ [43] [44].

Matlab and C++ were the two choices left after the first decision because of familiar in syntax and good performance. However, Matlab is chosen to be the programming language for this project at last. This is because it has a large library of in-built functions for image processing. This makes the developing work much easier. Furthermore, it also supports lots of matrix calculation, which is very convenient for developing this program that has lots of matrix related calculations. On the other hand, Matlab has a much slower execution time than using C++. However, as this project is a research and development project, and it should mainly concentrate on the research section, Matlab is chosen for the development of this project.

3. Theory that governs Iris Recognition

3.1 Anatomy and Physiology of the Iris

The iris is a protected internal organ of the eye, located behind the cornea and the aqueous humour, but in front of the lens. It is seen in cross-section in the anatomical drawing above. It is the only internal organ of the body that is normally visible externally. Images of the iris adequate for personal identification with very high confidence can be acquired from distances of up to about 3 feet (1 meter).

The visible features of an iris arise in the trabeculum, a meshwork of connective tissue that displays arching ligaments, crypts, contraction furrows, a corona and pupillary frill, coloration, and sometimes freckles. The striated anterior layer covering the trabecular meshwork creates the predominant texture seen with visible light, but all of these sources of radial and angular variation taken together constitute a distinctive "fingerprint" that can be imaged from some distance.

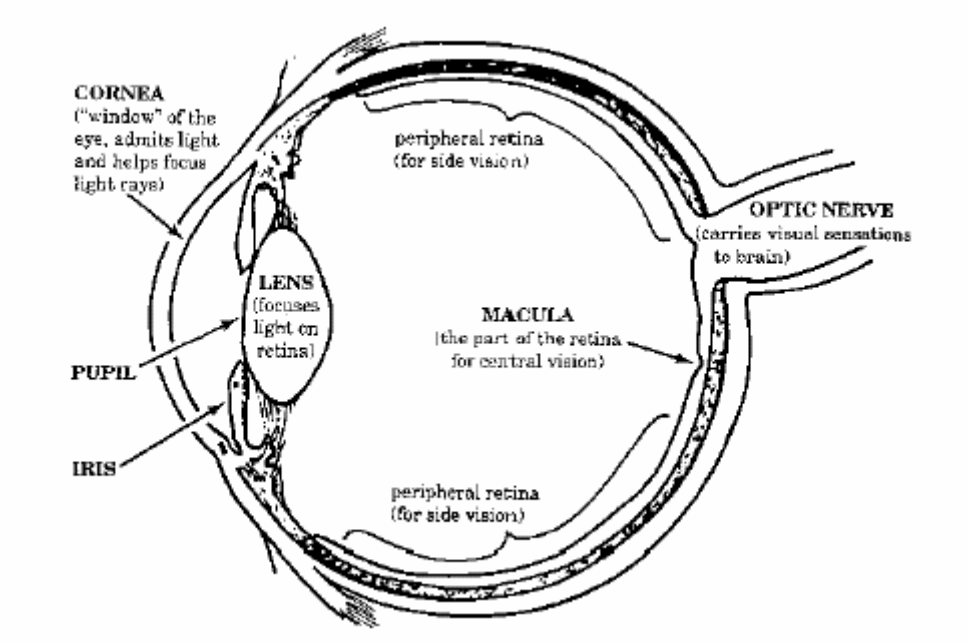

Figure 3-1The cross section of the Iris

A property the iris shares with fingerprints is the random morphogenesis of its minutiae. Because there is no genetic penetrance in the expression of this organ beyond its anatomical form, physiology, color and general appearance, the iris texture itself is

stochastic or possibly chaotic. Since its detailed morphogenesis depends on initial conditions in the embryonic mesoderm from which it develops, the phenotypic expression even of two irises with the same genetic genotype (as in identical twins, or the pair possessed by one individual) have uncorrelated minutiae. In these respects the uniqueness of every iris parallels the uniqueness of every fingerprint, common genotype or not. But the iris enjoys further practical advantages over fingerprints and other biometrics for purposes of automatic identification, including: the ease of registering its image at some distance from a Subject without physical contact, unobtrusively and perhaps inconspicuously; its intrinsic polar geometry, which imparts a natural coordinate system and an origin of coordinates; and the high level of randomness in its pattern, creating inter-Subject variability spanning about 250 degrees-of-freedom, and an entropy (information density) of about 3.2 bits per square-millimeter of iris tissue.

Developmental Morphogenesis and Chromatic Properties

The human iris begins to form during the third month of gestation. The structures creating its distinctive pattern are complete by the eighth month of gestation, but pigmentation continues into the first years after birth. The layers of the iris have both ectodermal and mesodermal embryological origin, consisting of (from back to front): a darkly pigmented epithelium; pupillary dilator and sphincter muscles; heavily vascularized stroma (connective tissue of interlacing ligaments containing melanocytes); and an anterior layer of chromataphores and melanocytes with a genetically determined density of melanin pigment granules. The combined effect is a visible pattern displaying various distinctive features such as arching ligaments, crypts, furrows, ridges, and a zigzag collarette.

Iris color is determined mainly by the density of the stroma and its melanin content, with blue irises resulting from an absence of pigment: longer wavelengths differentially penetrate while shorter wavelengths are reflected and scattered, a phenomenon resembling that which makes the sky blue. The heritability and ethnographic diversity of iris color have long been studied, but until the present research, little attention had been paid to the achromatic pattern complexity and textural variability of the iris among individuals.

3.2 Iris Recognition

The iris is an externally visible, yet protected organ whose unique epigenetic pattern remains stable throughout adult life. These characteristics make it very attractive for use as a biometric for identifying individuals. Image processing techniques can be employed to extract the unique iris pattern from a digitized image of the eye, and encode it into a biometric template, which can be stored in a database. This biometric template contains an objective mathematical representation of the unique information stored in the iris, and allows comparisons to be made between templates. When a subject wishes to be identified by an iris recognition system, their eye is first photographed, and then a template created for their iris region. This template is then compared with the other templates stored in a database until either a matching template is found and the subject is identified, or no match is found and the subject remains unidentified.

Although prototype systems had been proposed earlier, it was not until the early nineties that Cambridge researcher, John Daugman, implemented a working automated iris recognition system [49][26]. The Daugman system is patented and the rights are now owned by the company Iridian Technologies. Even though the Daugman system is the most successful and most well known, many other systems have been developed. The most notable include the systems of Wildes et al. [51][52], Boles and Boashash [53], Lim et al. [54], and Noh et al. The algorithms by Lim et al. are used in the iris recognition system developed by the Evermedia and Senex companies. Also, the Noh et al. algorithm is used in the 'IRIS2000' system, sold by IriTech. These are, apart from the Daugman system, the only other known commercial implementations.

The Daugman system has been tested under numerous studies, all reporting a zero failure rate. The Daugman system is claimed to be able to perfectly identify an individual, given millions of possibilities. The prototype system by Wildes et al. also reports flawless performance with 520 iris images [52], and the Lim et al. system attains a recognition rate of 98.4% with a database of around 6,000 eye images.

Compared with other biometric technologies, such as face, speech and finger recognition, iris recognition can easily be considered as the most reliable form of biometric technology [49]. However, there have been no independent trials of the technology, and source code for systems is not available. Also, there is a lack of publicly available datasets for testing and research, and the test results published have usually been produced using carefully imaged irises under favorable conditions.

3.3 Daugman's Algorithm

3.3.1 Overview of the algorithm

Daugman's algorithm is based upon a statistical test of independence. First, a grayscale iris image is captured from a near-infrared (NIR) camera. Then, after locating the iris within that image, the iris is normalized to allow for distortion from pupil dilation and the varying range of image acquisition. This normalized image is projected onto a set of Gabor filters to extract the phase information from the image, which is then quantized into a bit code. Noisy areas of the image have mask bits cleared for the affected area to ensure that this noise does not influence identification. The bit code thus generated is then compared to stored codes. The mask bits from the input and stored codes are used to neglect noisy areas. Finally, a test of statistical independence compares the percentage difference between the input code and stored image to a preset threshold. If the value is less than this threshold, the irises are determined to be matching [4] [56] [57]. Figure 3-2 contains a flow chart describing this algorithm.

Daugman's algorithm has the following **basic steps**:

- Image Acquisition
- Acquisition of Iris Image
- Location of Pupil and sclera boundaries
- Normalization of acquired Image
- Projection of Normalized Image onto Filter
- Generation of Iris code
- Mask Bit Generation
- Comparison of iris code

*Mathematical Explanation of Iris Recognition***:** An "IrisCode" is constructed by demodulation of the iris pattern. This process uses complex-valued 2D Gabor wavelets to extract the structure of the iris as a sequence of phasors (vectors in the complex plane), whose phase angles are quantized to set the bits in the IrisCode[4]. This process is performed in a doubly-dimensionless polar coordinate system that is invariant to the size of the iris (and hence invariant to the imaging distance and the optical magnification factor), and also invariant to the dilation diameter of the pupil within the iris.

The demodulating wavelets are parameterized with four degrees-of-freedom: size, orientation, and two positional coordinates. They span several octaves in size, in order to extract iris structure at many different scales of analysis. Because the information extracted from the iris is inherently described in terms of phase, it is insensitive to contrast, camera gain, and illumination level (unlike correlation methods). The phase description is very compact, requiring only 256 bytes to represent each iris pattern, plus control bytes that exclude artifacts such as eyelashes or reflections or data that is unstable or weak. The 2D Gabor wavelets are optimal encoders under the Heisenberg-Weyl uncertainty relation for extraction of information in conjoint spatial - spectral representations [4].

The recognition of irises by their IrisCodes is based upon the failure of a test of statistical independence. Any given IrisCode is statistically guaranteed to pass a test of independence against any IrisCode computed from a different eye; but it will uniquely fail this same test against the eye from which it was computed. Thus the key to iris recognition is the failure of a test of statistical independence. The equations and the wavelet phasor diagram below summarize the pattern encoding process. Using a Boolean XOR similarity metric on the phasor bit strings generates similarity scores among different IrisCodes that are binomially-distributed and that therefore have tails that attenuate extremely rapidly. More detailed information about the complex-valued 2D Gabor encoding wavelets, about the test of statistical independence, and the table of False Match probabilities is discussed later [4].

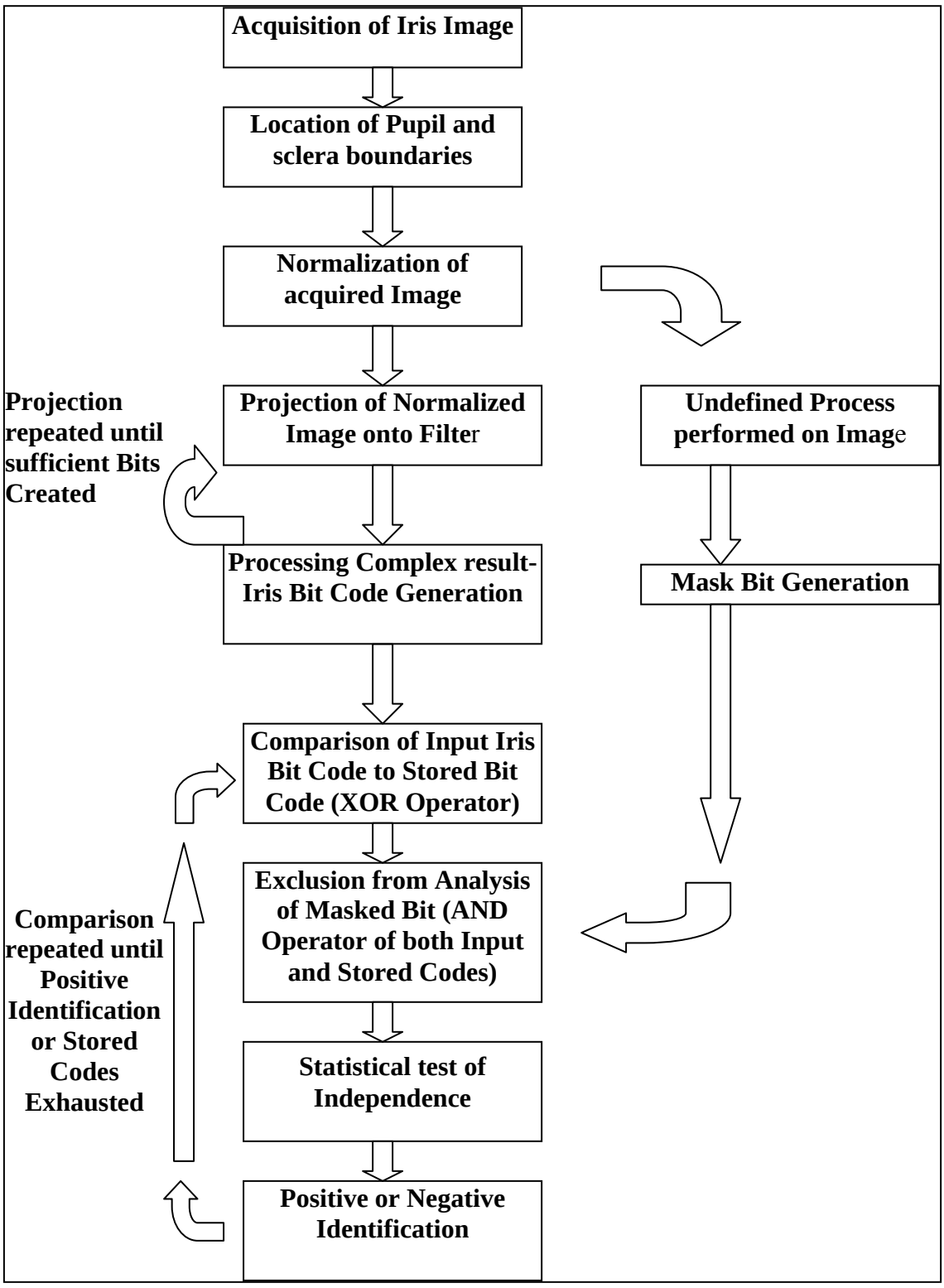

Figure 3-2 Flow Chart to show Basic Implementation of Daugman's Algorithm.

3.3.2. Location of the Iris

In order to locate the iris from within the eye, Daugman utilizes a circular edge detector of the form shown in equation (3.1).

$$\max_{(r,x_0,y_0)} \left| G_\sigma(r) * \frac{\partial}{\partial r} \oint_{(r,x_0,y_0)} \frac{I(x,y)}{2\Pi r} ds \right| \tag{3.1}$$

This edge detector involves estimating the centre of the edge to be detected, and by determining where the greatest change in intensity occurs can locate the sclera and pupil boundaries [4]. Figure 3.3 shows these boundaries. The blurring Gaussian, G. varies the value of σ, to obtain rough and then more precise locations for the boundary in an iterative process.

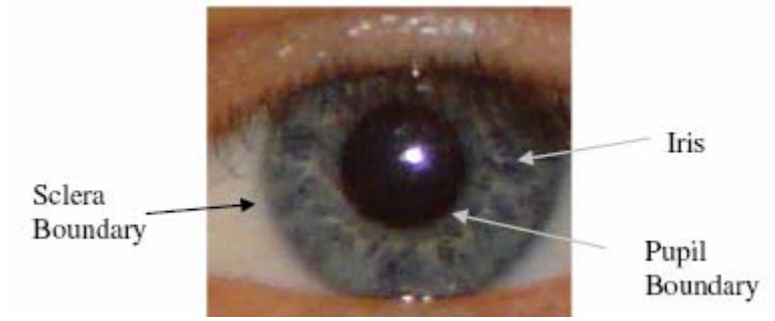

Figure 3.3 Boundaries, forms of Occlusion from Eyelids, Eyelashes, and Reflections.

3.3.3 Normalization of the Iris Image

Once the iris has been located, the iris needs to be separated from the pupil and sclera. In addition, to minimize the effect of pupil dilation and varying image sizes, the size of the iris image must be normalized. In order to normalize the image, Daugman utilizes a rubber sheet model as captured in equation (3.2).

$$\begin{aligned} &I(x(r,\theta).y(r,\theta)) \rightarrow I(r,\theta) \\ &x(r,\theta) = (1-r)x_p(\theta) + rx_s(\theta) \\ &y(r,\theta) = (1-r)y_p(\theta) + rx_s(\theta) \end{aligned} \tag{3.2}$$

The model stretches the points defined by the pupil (x_p. y_p) and sclera (x_s, y_s) boundaries to create a dimensionless coordinate system [4]. This can best be visualized by imagining making an incision radially through the iris, taking the two edges of the incision and pulling them until the result is a rectangle the dimensions of which vary from 0 to 2Π in the angular direction and from 0 to 1 radially. This process clearly then involves the stretching of the inner boundary more than the outer boundary, followed by stretching or compression in both the radial and angular directions to fit the rectangle into the new dimensionless system. As the pupil is not located in the centre of the iris, regions where there is a shorter distance between the pupil and sclera boundaries will be radially stretched more than regions where there is a greater distance.

By stretching or compressing the iris radially to fit the dimensionless coordinate system, pupil dilations, which can be approximated as a linear transformation [4], can be disregarded when attempting to recognize irises. The other advantage of this resizing is that the size of the iris in the captured image is no longer a factor, as long as the captured image has sufficient resolution.

3.3.4 Projection onto a Gabor Filter and Generation of the Iris Code

In order to filter the image, Daugman utilizes a polar version of the 2-D Gabor filter as shown in equation (3.3). A Gabor filter is essentially a Gaussian modulated by a complex exponential.

$$G(r,\theta) = e^{-i\omega(\theta-\theta_0)} \cdot e^{-(r-r_0)^2/\alpha^2} e^{-(\theta-\theta_0)^2/\beta^2} \tag{3.3}$$

The parameters r_o and θ_o determine the location of interest within the iris image. The size of the filter is determined by β in the radial direction and in the angular direction. The frequency term, ω, determines the frequency of the modulation of the complex exponential. The normalized iris image is projected onto the filter [4]. Figure 3.4 shows the real component of a Gabor filter.

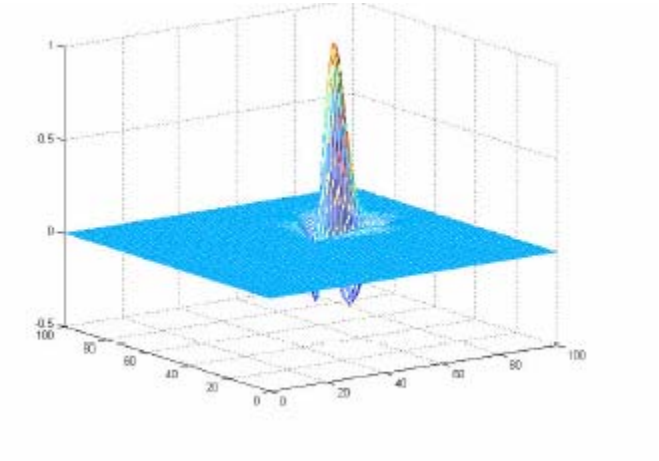

Figure 3-4 The Real Component of a Gabor filter

When used as filters, Gabor filters have a number of advantages. Gabor filters are resistant to intensity variation between images [58]. Gabor filters are also used effectively in the de-blurring of images [59]. However, the Gabor filters are not used to filter the image here. The filters are simply used as the angular oscillations in the filter can represent the striations in the iris pattern. Gabor filters are effective for this task, with Daugman observing that even highly blurred iris images produce distinct iris codes. This is critical in avoiding falsely matching blurred images to one another [56].

One disadvantage to Gabor filters is that the real component of the filter contains a non-zero gain at DC. This DC component can increase the dependence of the iris code on the image intensity. Daugman removes this component before using the filter [4].

The result of the projection of the normalized iris image onto the Gabor filter is a complex number. Daugman then quantizes the phase information of this number by representing the quadrant in which the number lies as a two bit binary number. That is, if the real component is positive, the first bit is set to 1, and if the imaginary part is positive, the second bit is set to 1. Conversely, negative values result in a 0. By quantizing this phase information Daugman allows for comparisons to be made very quickly between iris bit codes. In addition, by discarding magnitude information the iris codes become less affected by the intensity of the image. A 2048 bit code is generated for comparison [4].

3.3.5 Generation of Mask Bits

Based on some undisclosed method, Daugman generates one mask bit per iris code bit. A 0 in the mask bit sequence represents a section of the iris bit code that should be ignored due to noise, such as specular reflection, eyelid occlusion or eyelash occlusion [4]. This allowed Daugman to use a larger portion of the iris, whereas previously he had been forced to eliminate areas, such as the lower 90 degrees of the iris, from analysis because of the likelihood of noise [4], [56].

3.3.6 Comparison of Iris Codes to Determine Identity

In order to compare the iris bit codes, Daugman utilizes Hamming distances [4]. A Hamming distance is essentially the number of bits that differ between two sequences [10]. First, the two iris bit codes that are to be compared combined via the "exclusive or" (XOR) logic operator. Then, the two mask bit sequences are logically anded (AND) to this result to eliminate from the results any noisy areas. The number of l's in this resultant is divided by the total number of valid bits, (excluding masked bits), to provide a proportion of non- matching bits to total bits.

As phase information is being encoded, head rotation will change the phase and thus the resulting bit code. However, as each bit generated is associated with a particular angle, providing that the code has been structured correctly, the iris bit code can be shifted left and right to reverse this rotation. The degree of head rotation is never known, simply, the shift that produces the lowest Hamming distance is used for comparison [56].

The distance is compared to a preset tolerance. The higher this threshold, the lower the chance of false rejection. However, as the threshold increases, the chance of falsely accepting an individual also increases [4]. In this way, the security level of the system can be set to an appropriate balance between avoiding inconveniencing legitimate users, while maintaining security.

3.3.7 Accuracy of the System

Daugman's reported accuracy has increased with time, possibly as a result of improvements within the system. As mentioned previously, the accuracy of the system is dependant on the balance between acceptable false accept and false reject rates. Daugman recommends a distance of 0.32 [4]. Based on the most recent data, that corresponds to a 1 in 26 million chance of false acceptance [56]. Conversely, a 1 in 151 000 chance exists of a false rejection [4]. This clearly allows for the use of very large databases with a very small chance of error. Table 3.1 shows the chance of falsely identifying someone as the

Hamming Distance Threshold	Probabilities of False Acceptance
0.26	**1 in 1.00 x 10^{13}**
0.30	**1 in 1.50 x 10^{9}**
0.33	**1 in 4.00 x 10^{6}**
0.35	**1 in 1.33 x 10^{5}**
0.40	**1 in 1.70 x 10^{2}**

Table 3-1 Probability of a False Match for Various Hamming Distance Thresholds

3.4 The Iris Databases

In order to develop and implement Daugman's algorithm the iris databases were required. A near-infrared iris image database of CASIA [61] and a color iris image database [62]. The color images database is downloaded from UBRIS. [62]

3.4.1 CASIA

The CASIA Iris image database provided the near-infrared image database [61]. It is an image database consisting of images of 108 different iris images acquired by a digital optical sensor. Each iris is photographed 3 times in an initial session and then a further 4 times in a second session at a later date. For the CASIA database, because all the images are taken using specific designed NIR camera there is no reflection dot located in the pupil region. The database mainly contains the irises of people of Asian extraction [61]. From the CASIA images, however, it is clear that the dark pigmentation common among this ethnicity does not have any real noticeable affect on the images captured.

3.4.2 UBIRIS

Despite the fact that many of the iris recognition approaches obtain almost optimal results, they do it under particularly favorable conditions, having few image noise factors. These conditions are not easy to obtain and require a high degree of collaboration from the subject, subjecting him to slower and uncomfortable image capture processes. The aim of UBIRIS is related with this point: it provides images with different types of noise, simulating image captured without or with minimal collaboration from the subjects, pretending to become an effective resource for the evaluation and development of robust iris identification methodologies.

UBIRIS [62] database is composed of 1877 images collected from 241 persons during September, 2004 in two distinct sessions. It constitutes the world's largest public and free available iris database at present date. I have downloaded for my research purpose all the three sets with permission from their websites.UBRIS database used a Nikon E5700 camera with software version E5700v1.0, 71mm focal length, 4.2 F-Number, 1/30 sec. exposure time, RGB color representation and ISO-200 ISO speed. Images dimensions were 2560x1704 pixels with 300 dpi horizontal and vertical resolution and 24 bit depth. They were saved in JPEG format with lossless compression. For the first image capture session, the enrollment, tried to minimize noise factors, especially those relative to reflections, luminosity and contrast, having installed the framework represented as in figure 3-5 below inside a dark room.

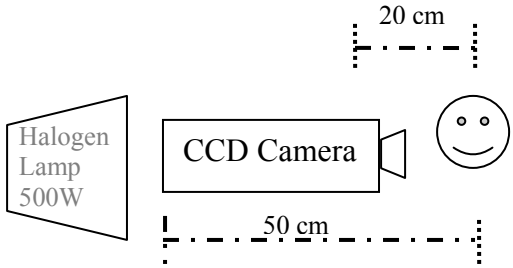

Figure 3-5 Image capture framework

In the second session [62] changed the capture location in order to introduce natural luminosity factor. This enabled the appearance of heterogeneous images with respect to reflections, contrast, luminosity and focus problems. Images collected at this stage pretend to simulate the ones captured by a vision system without or with minimal active collaboration from the subjects. These noisy images will be compared to the ones collected during the enrollment stage

3.5 Other Iris Recognition Systems

Masek performs a thorough review of existing iris recognition techniques, from both commercially implemented and not commercially implemented systems [39]. However, Masek fails to find any significant advantages in any of the existing systems available over Daugman's techniques. Many utilize intensity dependant processing techniques, such as the Hough transform. In addition, Daugman's system has been thoroughly tested by himself using large databases [56] and also independently, with smaller databases and a mildly modified algorithm, by Masek [39].

A significant amount of material is readily available on Daugman's algorithm. Mainstream textbooks contain information on Daugman's work [53]. Daugman's work is both fast and accurate, and also being largely well documented. Thus, it is hard to justify spending time implementing other systems. As a result, after initial research, other systems were discarded.

4. Implementation

The initial step in attempting to successfully implement an iris recognition system was to replicate Daugman's basic iris recognition system. As mentioned in previous sections, this involves the acquisition of a grayscale iris image and the subsequent processing and comparison of that image to iris codes stored in a database to attempt to identify an individual.

This system was implemented utilizing MATLAB. While MATLAB is slower than a lower level language, such as C or C++, the built-in functions, such as convolution and the Discrete Fourier Transform as well as matrix representation which was heavily used in this project, significantly reduced development time.

Solutions to Undefined Areas of Daugman's Algorithm:

Within Daugman's Algorithm, a number of stages of his algorithm have not been clearly defined. In addition, while Daugman provides a number of equations for techniques his algorithm is reliant on, often the values of the constants used within those equations are not defined.

4.1 Location of the eye Socket

Even though localizing eye socket is not considered in Daugman's Algorithm, this project mainly focuses on the steps after image acquisition. It can be noted that the difficulty in locating the eye socket can be minimized by having well established database of Iris Images for research purpose. Inserted colored dots around the eye to assist in location. Given the goals of this project, it was determined early on that this project would not attempt to resolve this issue, but instead focus on locating the iris once the eye socket has been located. For details of Shifting look at section 4.9 which tries to shift matrix in order to compensate the tilt of human position.

4.2 Localizing Pupil and Iris

The localization of the pupil and iris is the first section of the iris recognition system. The center point of the pupil and iris are different and their radius sizes are different. Therefore two separate searching are needed to locate the iris and the pupil. However, the algorithm to find the iris and pupil are nearly the same, with some differences in the threshold values. From Daugman's algorithm for iris recognition, he used a method called Integro-differential operator (Equation 3.1) to detect the boundaries of this iris and pupil. Which is a circular edge detector to determine the boundary between the sclera and the iris and also the iris and the pupil (refer to equation (3.1). However, the pupil boundary and sclera boundary are not concentric. The equation requires a process of estimation of the central point of the sclera boundary circle and the pupil circle. This estimation is then improved in some undefined iterative method as the parameter σ is varied.

It is a circular edge detector; the basic algorithm is to find the maximum intensity change with different radius from a center point. This equation can be used because the iris and the pupil are approximated as circles. However, in Daugman's paper, he did not mention about how to find the parameters for his algorithm on iris detection. In order to implement his algorithm, the values of x_0 and y_0 need to be found. This is because the position of the data, a reference center, must first be defined to enable the search on the pupil and the iris boundaries. This comes to another problem that the reference center is not necessarily the actual center. Therefore, the reference center must be verified as a good approximation to the actual center. As a result of that, the localization process is separated into three separate sections,

i. Find a starting point,
ii. Find the estimated boundaries.
iii. Verify the current location and improve it if needed.

The flow chart of this process is shown:

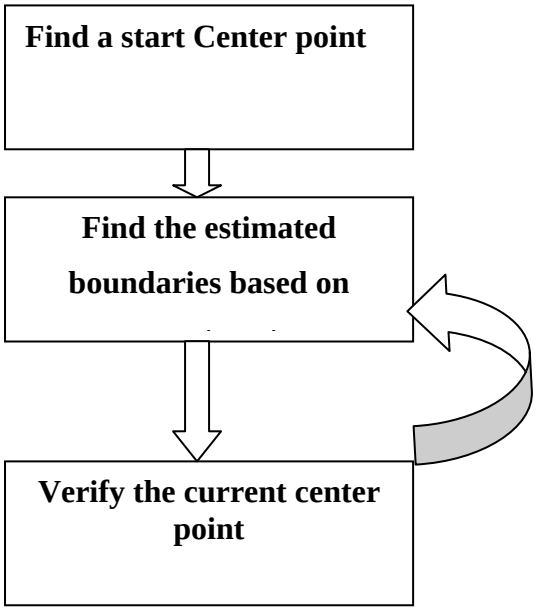

Figure 4-1. Flow chart of over all process of the Iris Extraction.

For the CASIA images, he pupil to iris boundary presented a much more significant intensity change than the iris to sclera boundary. As a result, the location of the pupil was determined before the location of the iris.

In order to find an initial estimate of the centre of the pupil, the intensity of the iris image was summed two separate times, horizontally and vertically. The minimum of these summations represent the x and y coordinates of the initial estimate of the centre. This centre was then used in equation (3.1) to determine the radius to the boundary from that centre point. *sum(I)* function returns a matrix, which is a row vector with the sum over each column. And the *sum(I')* is row vector over each of row. Find gives the index value of this minimum value and there I start as original point of search. Where I is the intensity of the image and I' is the inverse.

```
index_x = find (sum(I) = =  min(sum(I)));
index_y = find (sum(I') = = min(sum(I')));
```

(Excerpt of Matlab code.....)

For the CASIA database, because all the images are taken using specific designed, NIR camera there is no reflection dot located in the pupil region. As a result of that, the method in finding the estimated center is discarded. Previous method using the center point as the center is used again to find the first center point for the boundary searching. However, it will have a large effect on the final result of this section. An example is shown in figure 4.2 where the point is around the boundaries, it is hard for it to decide

the position to move to and this creates a large error rate for the final estimated center point.

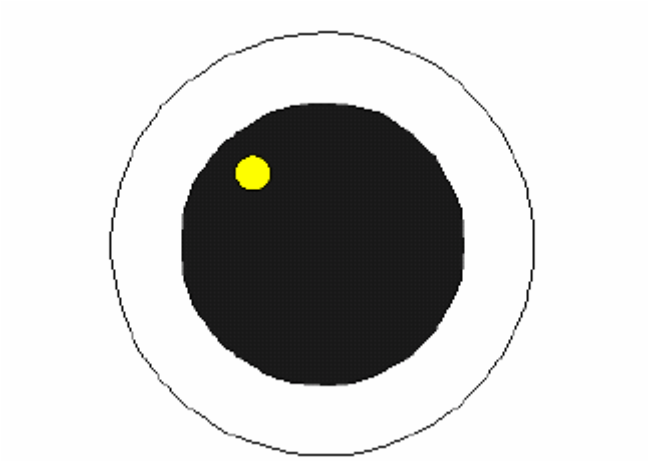

Figure 4-2 shows the position of the search point where problem is likely to occur

This can be easily seen from the following two graphs which show intensity of column and rows. Graphs of the sum in intensity in both horizontal and vertical directions are shown

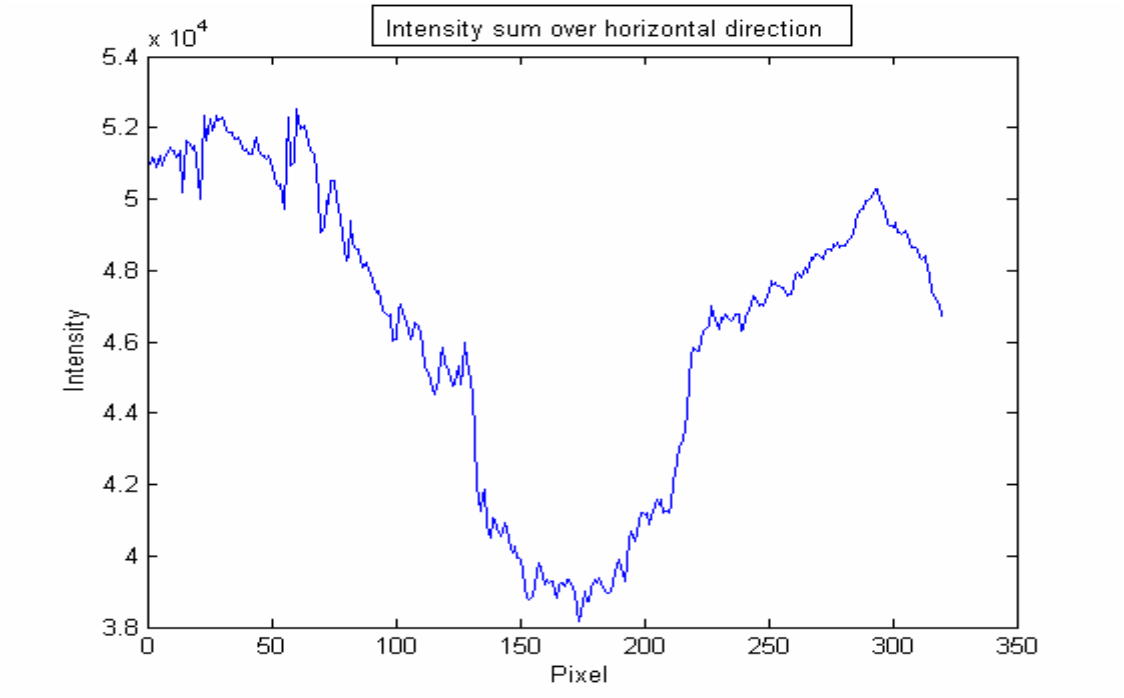

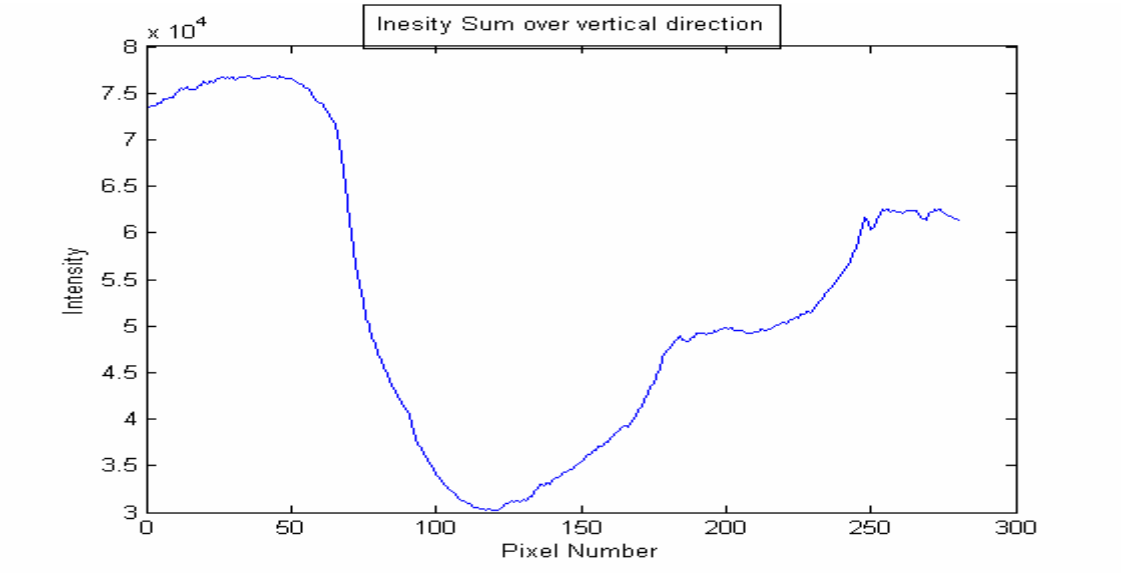

Figure 4-3 Intensity sum over a) Horizontal and b)Vertical

In order to verify that this is indeed the centre, 6 to 8 nearby locations were also used as centers for equation (3.1). See Figure 4-1 for details. If the original centre was a good estimate of the actual centre of the pupil, then the nearby test points would be expected to also be reasonable approximations to the centre. This was tested by checking the radius to the boundary and the intensity change at the boundary of the test points.

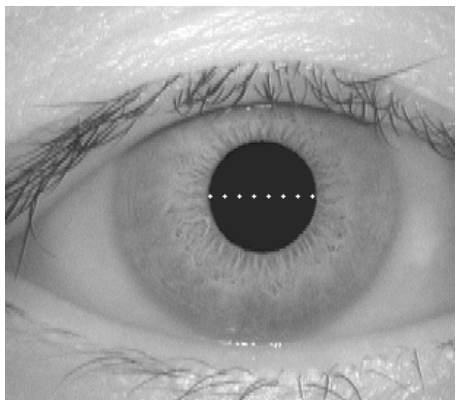

Figure 4-4. The eight points selected

These points are I(i,j) to I(i,j + 60) with 10 in j-direction and finally I(i,j+90). If these values fell within an acceptable range for a particular test point, that point was declared a good or 'valid' test point. If the majority of the nearby test points were valid, the estimated centre was determined to be a valid centre. If this was not the case, the estimated centre was moved in the direction of the most valid test locations. In the absence of any test locations being declared valid, the estimated centre moved in the

direction of the highest intensity gradient at the boundary. This process was repeated until a valid centre was found. Various pattern detectors helped.

4.2.1 Algorithm to find the pupil

Estimating the center, the first rough estimates:

In order to estimate the center of the pupil I look for 6-8 pixels which their gray scale is under than 65 in equal gaps.(10 pixels). The constant 65 is chosen after examining a lot of pictures using Photoshop and Matlab. In above mentioned way, the rough position is determined and I have taken its center to be the estimated center of the circle.

Finding the accurate center:

1. To find the center of the pupil accurately the rectangle is chosen around the estimated center and I assume that every point in it can be the center of the pupil. (see Figure 4-2 below)
2. To every point in the rectangle start draw circles from a minimum radius to a maximum one.
3. Mean every circle and keep its value.
4. Gradient is calculated
5. Finding the gradient
    a. Subtract the mean value of every circle from his neighbor and find the maximum result. This maximum result is the gradient for the specific point.
    b. Do this steps to all the points in the rectangle.
    c. Take the maximum result (gradient) for all the points in the rectangle.
    d. The gradient is the radius and the center of the pupil.

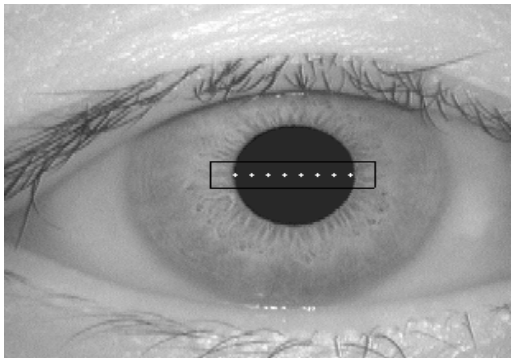

Figure 4 -5 Rectangular Search point

4.2.2 Algorithm to find the Iris

The same steps to find the pupil with minor adjustment implemented find the iris extraction. A major problem exists when I try to find the iris in the algorithm described. When mean of the gray levels performed on the circle sometimes biased slightly from the true result. This happens due to the eyelashes which has lower mean value and detection of the iris imperfect:

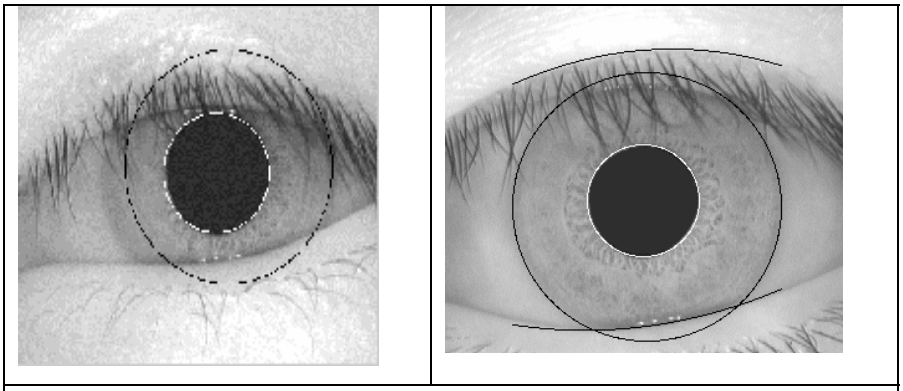

Figure 4-6 Example of an imperfect (left) & perfect (right) detection

In order to solve this problem two prior steps were followed:

1. Mean the circle from 0-360 degrees as I did for the pupil but here I mean from 180-225 degree, and from 325-360 degree. This method prevents the eyelashes to influence because they are hardly present there. These two pies lie on the third and fourth Quadrants of the Iris. Where by there are only pupil, iris and sclera of the image as shown in the following figure 4-7.

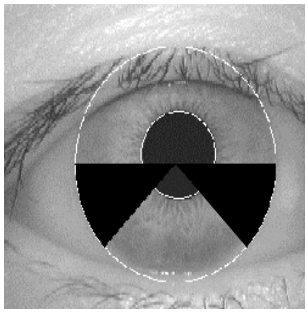

Figure 4-7 - The searching region

2. Median filter and Gaussian filter done on the signal to drop off the noise as eyelashes influence the mean gray level.

The blur factor of the equation is found from a number of testing. Originally, the color database is used to develop the system. The difference between the acceptable pupil range and the iris range is around 10 pixels. Therefore, a series of testing from a blur factor of 1-10 is performed. The blur factor is the factor that the signal will be smooth out by the Gaussian function, in other terms; it also means the frequency range that the Gaussian function will cover. After a series of testing, it is found that the blur factor of size 5 will be the best to use. This is because if the blur factor is too large, the signals is smoothed too much and if the blur factor is too small, the oscillation of the signal is too large, so it is hard to detect the maximum or local maximum region.

The process is quite different for the two databases due to the intensity difference on the iris region. The location of the boundary can be found based on the intergo-differential equation mentioned above; however, the meanings of those boundaries depend on the color of the image.

Generally that equation is used to detect the change in intensity. The areas that have the large change in intensity will be the pupil boundaries and the iris boundaries. However, depending on the eye color of the person, the maximum change in intensity will be located in different regions. If the person has light colored eyes, e.g. blue color, the largest change in intensity will occur in the pupil boundary. If the person has dark colored eye, the maximum change will locate in the iris boundaries. As a result of that, the intensity of the iris region will be used to determine if the input image is a dark colored eye or a light colored eye. Then if it is light colored eye, the maximum change will correspond to the lowest intensity. The iris boundary is found by finding the local maximum around a specific range. This range is known from observation to the images taken. The pupil generally has a size between 15-25 pixels and the iris generally has a size between 35-50 pixels in the color database. On the other hand, if the input image is a dark colored eye, the maximum change will correspond to the iris region and the pupil boundary will be found by searching the local maximum on the specific range.

The intensity change in the iris region and the white region is not as clear as the change between pupil region and the iris region. Therefore in order to detect the radius for the iris, there is a limit on the size of the iris. From Masek's research paper on the CASIA

database, the size of the iris radius varies between 85-150 pixels, a threshold value of 90-130 pixels set as the possible range of iris radius size. This is because this large range has a large effect on the accuracy on the iris detection process. In order to find the iris boundary, the local maximum around that range will be found. That local maximum corresponds to the iris boundary. See Figure 4-8 for details.

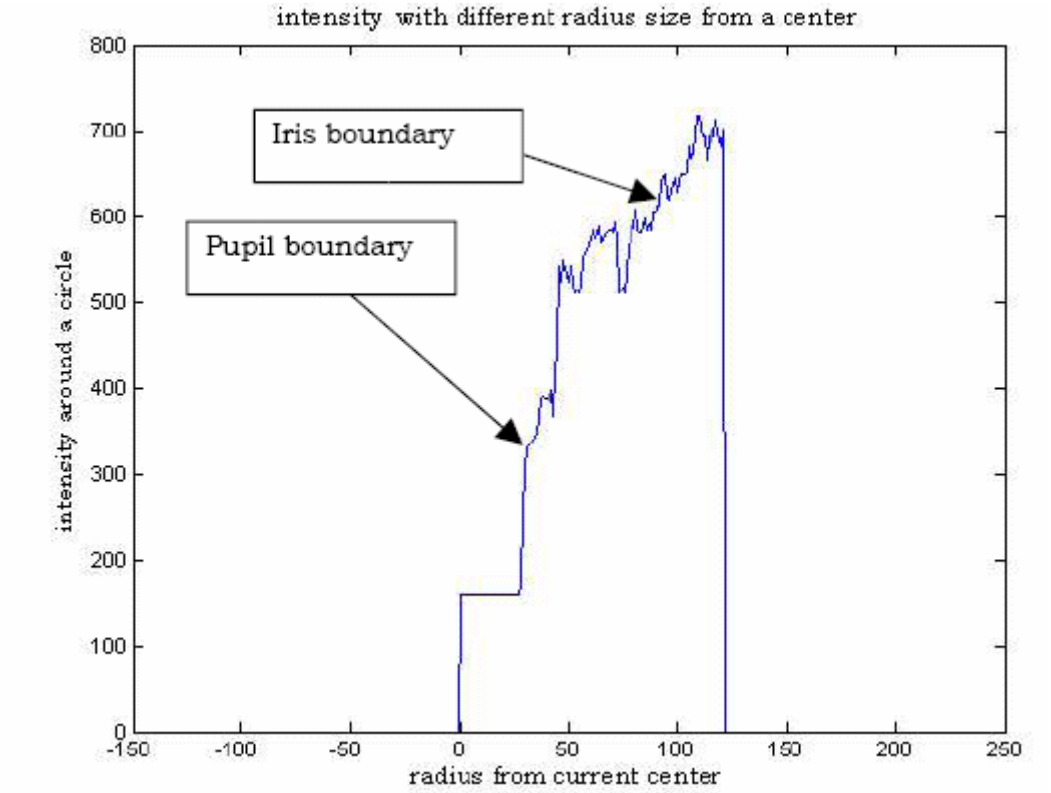

Figure 4-8 Sum of intensity with different radius from the current center

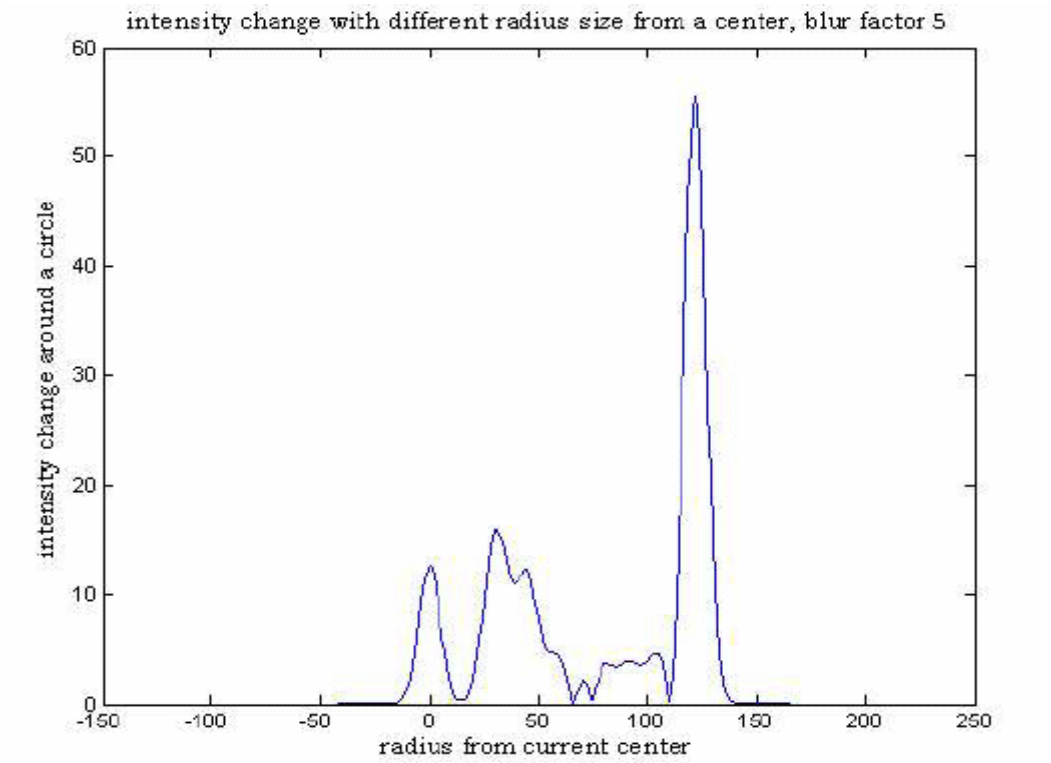

Figure 4-9 Intensity change with different radius from the center

4.2.3 Verifying the Estimate Center

After finish finding the estimated boundaries for iris and pupil, the location of the current center point must be verified as it is an good approximation to the actual center point or not. If it is not a good estimation of the actual center point, a new location must be found.

Daugman did not mention anything on this section. Therefore, a series of testing is first done to find the properties of the center point. Based on the testing results, the actual center generally has a property. That property is that the surrounding points around the actual center will have an estimated boundaries center within the acceptable range, and the size of intensity change will be larger than a threshold value. Therefore, an algorithm is defined.

The algorithm is to check 4 other possible test points surrounding the current center point. If all these points have a boundary size and intensity change larger than a threshold value, the center point will be classified as a good approximation to the actual circle. However, if it is not a valid center point then it is moved in the direction where the requirements agree. There is a priority given on some specific direction. The left direction will have a higher priority than right and up has a higher priority than down. However, there are a few problems on this algorithm. The testing position is easy to stop in one point and that point is not a valid center. The movement on the new position is biased because of the priority given. A diagram 4-10 shows the idea of the 5-point algorithm:

```
Rshift=[R(2:end) 0];
Rdiff=(Rshift-R);
Rdiff(ro_initial2-1)=0;
Rdiff(end)=[];
   ...
intens_max_x0_y0=max(Rdiff);
radius_max_x0_y0=find(Rdiff==max(Rdiff));
radius_max_x0_y0=radius_max_x0_y0(1,1);
RADIUS(y0,x0)=radius_max_x0_y0;
INTENS(y0,x0)=intens_max_x0_y0;
```

(Excerpt of Matlab code.....)

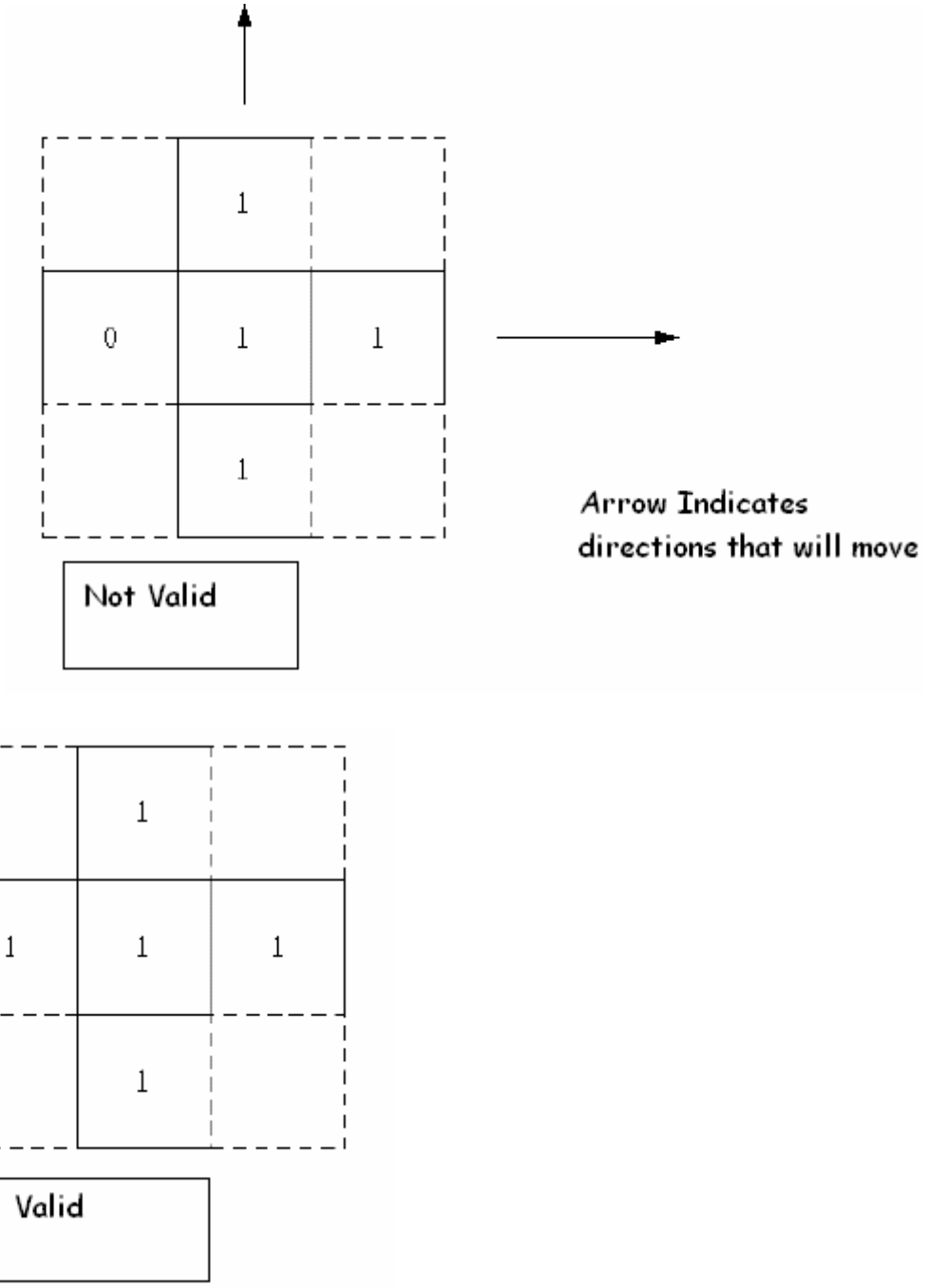

Figure 4-10. Five search points method.

Therefore, more test points can be created. As a result, this algorithm is to create 8 other test points around the current test center. For each of the test points, the boundaries detection mentioned in the above section will be performed. Two 3X3 matrices are created. The positions of those 8 points are all 7 pixels always from the center point. In those 3x3 matrices, the locations in the matrix correspond to the location of the point from the center point. The first matrix called valid will record the result from each check. That checking process is to check if the point has an estimated boundary and intensity change within the acceptable range. If it lies between the acceptable range for

the boundaries radius and the intensity change, 1 is stored in the matrix. If it fails to meet the requirement, 0 is stored in the matrix. For a valid center point, it must have at least 7 or more points in the matrix that scores a 1. If it does not meet that requirement, it is classify as an invalid point and a new location is created. The new location is created by moving the old location to the direction where the valid points are located. If there is no new position found, the new location will be found based on the other matrix. That matrix records the change in intensity at the boundaries on each location. It will move the center point to the direction where the intensity change is larger than a threshold value, i.e. 10 for iris boundary and 15 for pupil boundary. If a new location still cannot be found, the threshold for testing the intensity change will be decreased by 5. The diagram below shows the idea of the process.

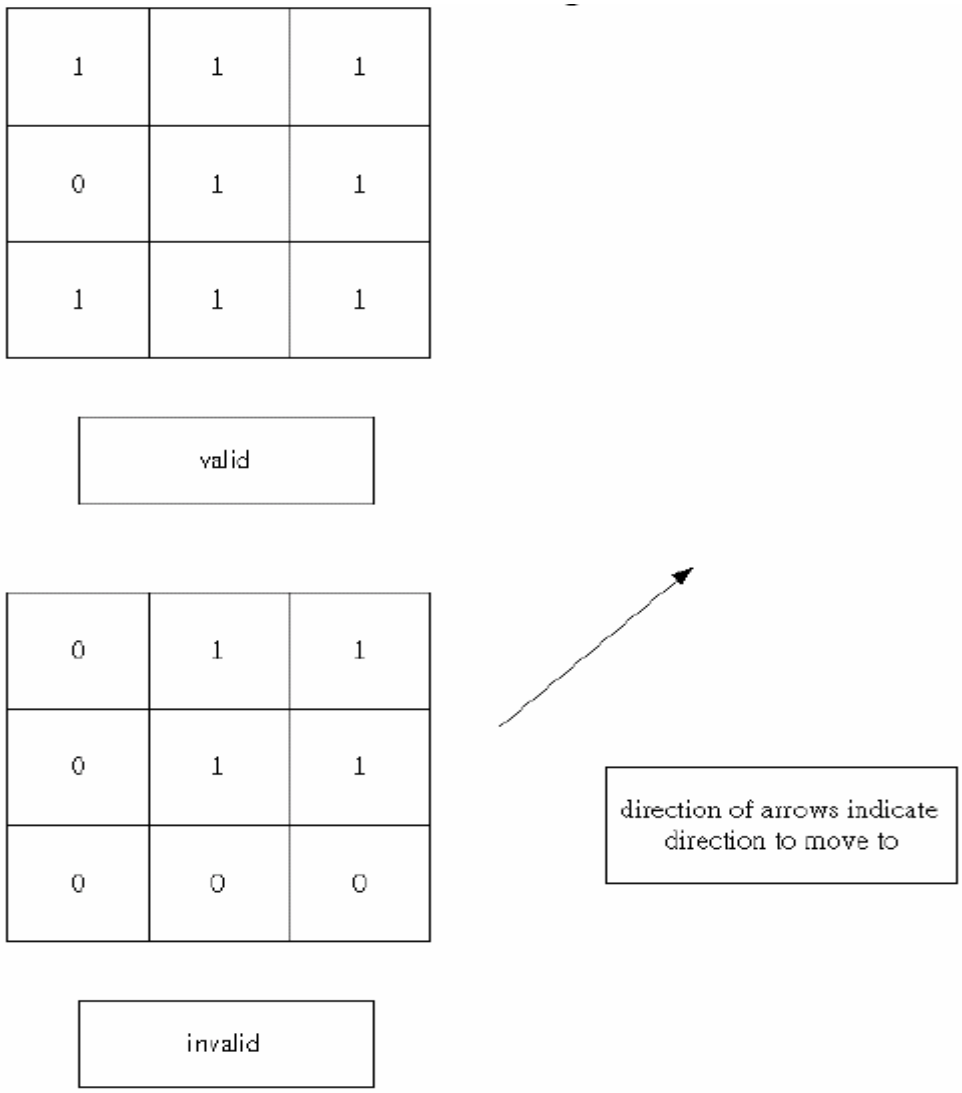

Figure 4-11 Case I, new position is found based on the valid matrix

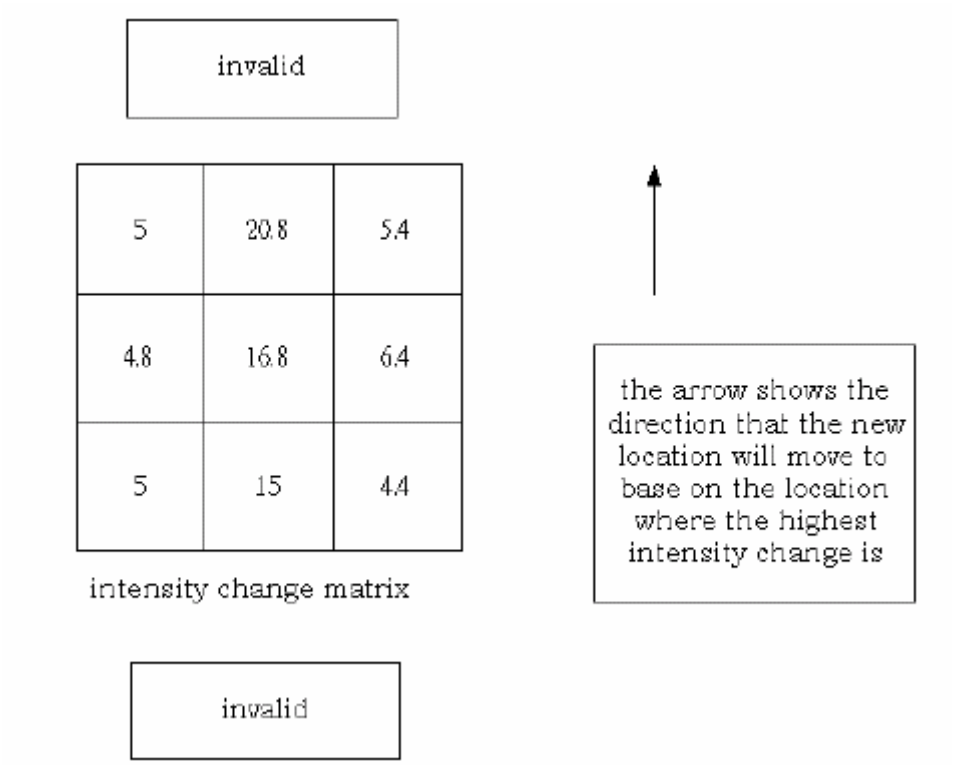

Figure 4-12 case II, when the new position cannot be found using the valid matrix

The program used to find the eyelash and eyelid. Masek also used a few algorithms to remove the sections of eyelids and eyelashes. First, his program finds the location of the iris and the pupil, and then based on this information; Canny edge detection and Hough transform are used to find the eyelid and masked off those area [2]. In order to remove the eyelid, here I checked for the intensity of the eye image, if any position has intensity larger than a threshold value, then that position is classified as an eyelash and it will be masked off.

In the next two section the my methods for finding upper and lower curves are discussed in details.

4.3 Finding the bottom curve

The Algorithm to find down curve:

1. In order to find the down curve I assumed that it behaves as a parabola.
2. Find the points that describe the parabola by using a wave which is called: Haar wave.
3. Choose columns in the iris area (9 for each side of the iris center) and make a convolution with every column and the Haar wave.
4. The result of every convolution is a number about 1 (inverted the gray scale from 0-255 to 0-1 gray scale) and the maximum result is the point I want.
5. Doing this convolution to all the columns to get the points for the parabola.

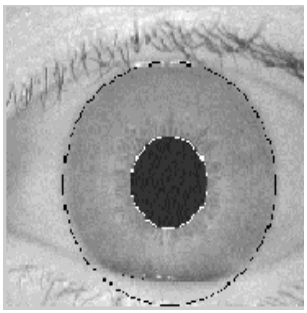

Figure 4 -13 - The detected points of the parabola

.

4.4 Finding the upper curve

Here there are two assumptions:

1. The eyelid is very close to a parabola.
2. Near the eyelid I have the largest arc gradient all over the picture.

The Algorithm to find up curve(arc gradient method) :

In order to find the up curve I developed a method called the arc gradient method, that is described as follows :

1. Search the curve in the upper half of the picture and start with an initial curve.
2. Pass over all possible parabolas in that region and the mean gray level of the picture in the coordinates of the parabola is the grade of the parabola.

3. Pass over the vertical axis and for every x0 take all the parabolas with the same parameters (a, b) and different c when c is shifted one pixel, and search for the gradient from one parabola to another.
4. The parabola at the point x_0 and with the parameters (a_0, b_0) that gives the largest gradient along the vertical axis is the desired one.

4.5 Normalizing the Image

In order to be able to compare the iris, it is dependant on a few factors. They are the size of the image, the location of the pupil, the size of the pupil and the iris. These factors cause a lot of problem before comparing the image. In order to get rid of the dependent factor and make it independent from the size factor, the rubber sheet describes above is used to solve the problem.

Firstly, the pupil is forced to move into the center position of the iris. This simply means to expand the section with the minimum distance to the iris boundary circularly and shrink the other side circularly to achieve this. This is shown in figure 4-14.

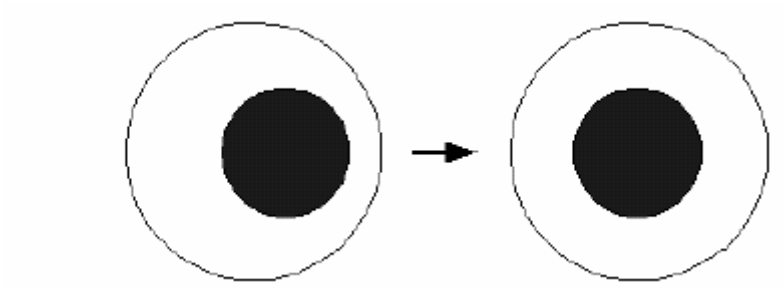

Figure 5-14 Pupil is moved to the center of the iris

After they are centered, both the iris and the pupil are resized to a standard size, therefore all the iris image inputted will be in the same size so that they can be compared

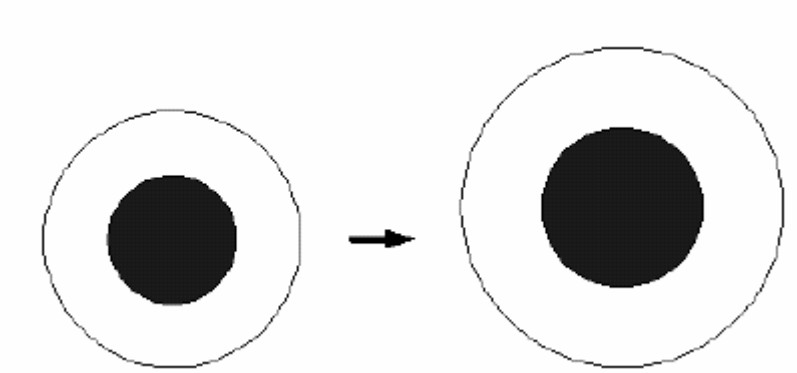

Figure 4-15. The iris and pupil boundaries are stretched to a standard size

Then the iris image is then cut at one point and stretched into a rectangular shape, for the horizontal axis it varies from 0 to 2Π, the vertical axis is from 0 to 1 in terms of ratio to the radius. The matrix to represent this rubbersheet is a 21 x 256 matrix. The outlook of the rubbersheet is shown in:

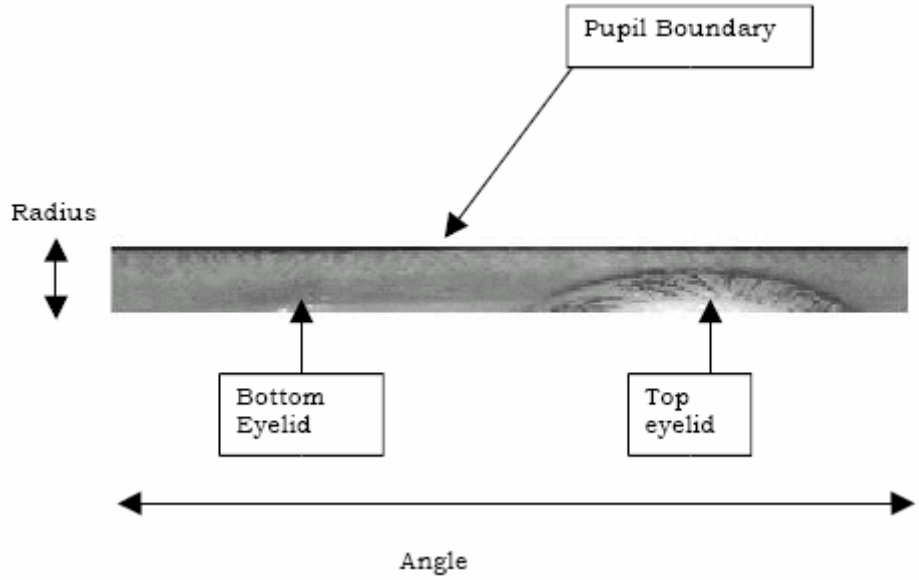

Figure 4.16 Iris image after the rubbersheet process

4.6 Mask Bit Generation

After the locations of the reflection, eyelid and eyelashes are found, the matrix of the reflection and the matrix of the eyelid and eyelashes will be combined using the OR functions. This means that the two matrices will be combined into a single matrix. The matrix is then converted to a rubber sheet image. This rubber sheet image is then used to generate the 1x2048 mask bit matrix. In order to generate the mask bit matrix, the position and size of each filter need to be known. The positions of the filters as stated

before are separated into two separate directions, the vertical direction and the horizontal direction.

Because the position data is in a polar coordinates form when inputted to the program, this means the data are in radius size for vertical direction and the horizontal direction represents the angle. Therefore, the data is then converted back to the rubber sheet scale first. Mask bit can be generated afterwards by checking the range of coverage of the filter
with a specific position. If any of the data in that range contains a 0, then that the mask bit of that filter is set to 0, indicates that the data of that filter can be ignored. A detail image to show these procedure are shown in figure 4-17.

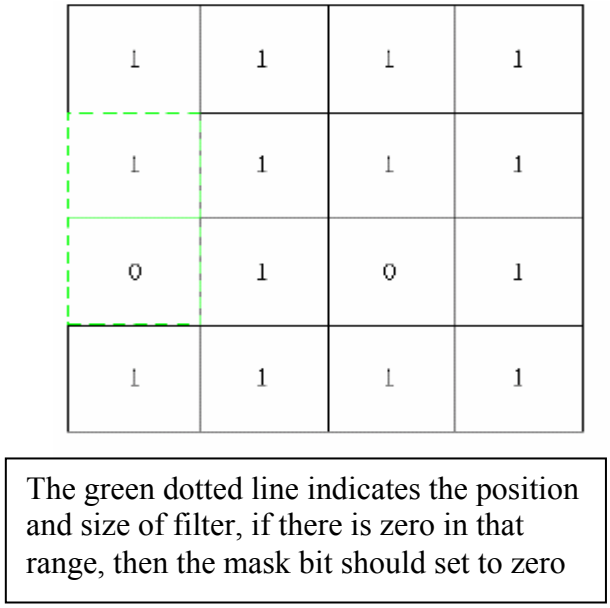

Figure 4-17 How to mask off the bit

Steps that describes the procedure to generate the mask bit is shown below:

1. Sometimes the eyelid of the eye which requests to enter is lower or higher than the one in the database. This can cause a huge difference in the samples I have, and the same person may get a rejection instead of permission.
2. To avoid that noise do masking. Every image has a mask besides the processed image

Figure 4-18 - The mask

The desired data is the black one.

3. The image (to be processed) , ORed with the masks

OR

=

Figure 4-19 - masking by or operation between two pictures to get the result in the third picture

4. After finding the common information Continue the process

4.7 Filtering with Gabor

After normalization the signal is convolved with matrix with one-dimension Gabor. As mentioned above, the Gabor filters are used to extract the iris information out. The Gabor filter is constructed by modulating the cosine and the sine wave with the Gaussian function. A signal is represented a quartered pair of Gabor Filter. The real part of the filter is represented by cosine wave and the imaginary part of the filter is represented by the sine wave. The real part is an even symmetry filter and the imaginary part is an odd symmetry filter. The phase information of the Gabor filter is quantized into four levels. That is the negative real and negative imaginary; negative real, positive imaginary, positive real and positive imaginary, positive real and negative imaginary. By representing the data in this way, the effect of the illumination is ignored.

Note that the conversion is cyclic and in one dimension. After the conversion I quantized the matrix result. The positive elements got the value '1' and the negative - '0'

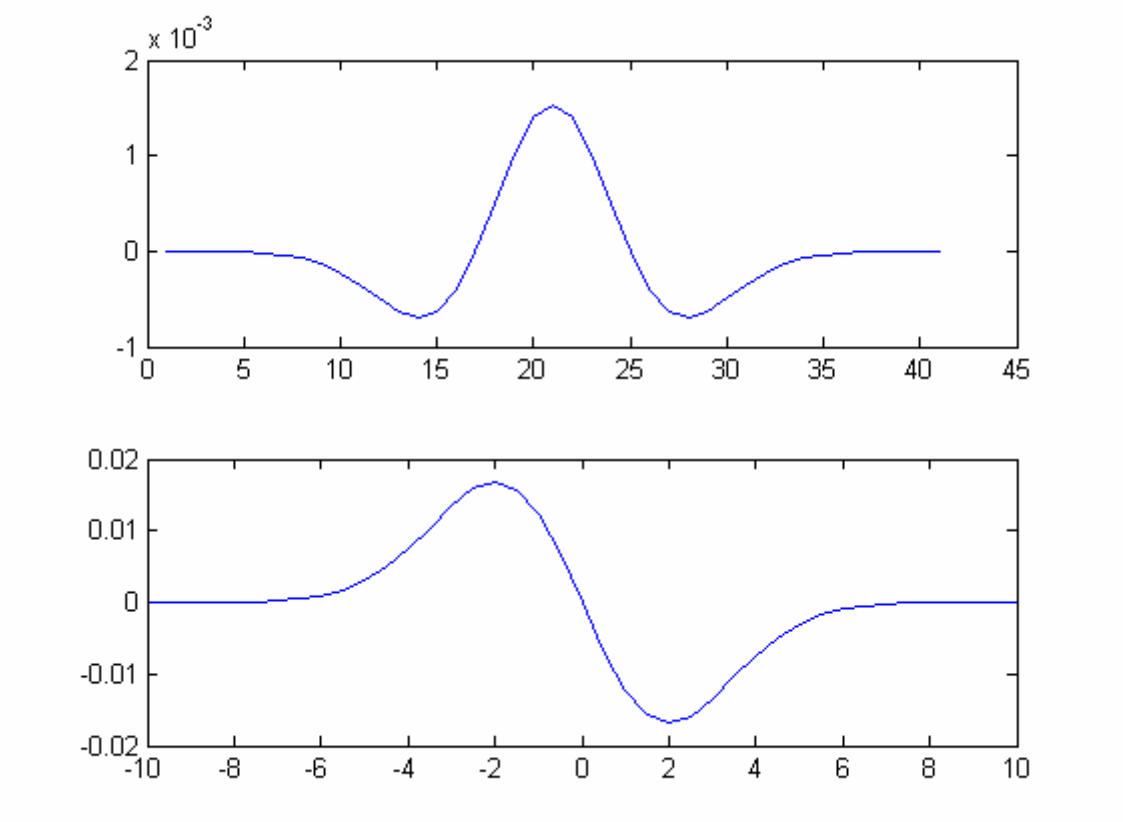

Figure 4-20. Gabor Function.

4.8 Comparing Codes

1. To compare between the codes (the matrixes) do XOR bit to bit.
2. If the eyes are different (different person) I got about 0.5, if it is the same person it is about 0.3.
3. The value I get is called HD.

The Hamming distance gives a measure of how many bits are the same between two bit patterns. Using the Hamming distance of two bit patterns, a decision can be made as to whether the two patterns were generated from different irises or from the same one.

In comparing the bit patterns *X* and *Y*, the Hamming distance, *HD*, is defined as the sum of disagreeing bits (sum of the exclusive-OR between *X* and *Y*) over *N*, the total number of bits in the bit pattern.

$$HD = \frac{1}{N}\sum_{j=1}^{N} X_j (XOR) Y_j \tag{4.1}$$

Since an individual iris region contains features with high degrees of freedom, each iris region will produce a bit-pattern which is independent to that produced by another iris, on the other hand, two iris codes produced from the same iris will be highly correlated.

If two bits patterns are completely independent, such as iris templates generated from different irises, the Hamming distance between the two patterns should equal 0.5. This occurs because independence implies the two bit patterns will be totally random, so there is 0.5 chance of setting any bit to 1, and vice versa. Therefore, half of the bits will agree and half will disagree between the two patterns. If two patterns are derived from the same iris, the Hamming distance between them will be close to 0.0, since they are highly correlated and the bits should agree between the two iris codes.

The Hamming distance is the matching metric employed by Daugman, and calculation of the Hamming distance is taken only with bits that are generated from the actual iris region.

For matching, the Hamming distance was chosen as a metric for recognition, since bit-wise comparisons were necessary. The Hamming distance algorithm employed also incorporates noise masking, so that only significant bits are used in calculating the Hamming distance between two iris templates. Now when taking the Hamming distance, only those bits in the iris pattern that correspond to '0' bits in noise masks of both iris patterns will be used in the calculation. The Hamming distance will be calculated using only the bits generated from the true iris region, and this modified Hamming distance formula is given as

$$HD = \frac{1}{N - \sum_{k=1}^{N} Xn_k (OR) Yn_k} \sum_{j=1}^{N} X_j (XOR) Y_j (AND) Xn'_j (AND) Yn'_j \tag{4.2}$$

where Xj and Yj are the two bit-wise templates to compare, Xn_j and Yn_j are the corresponding noise masks for Xj and Yj, and N is the number of bits represented by each template. Although, in theory, two iris templates generated from the same iris will have a Hamming distance of 0.0, in practice this will not occur. Normalization is not perfect, and also there will be some noise that goes undetected, so some variation will be present when comparing two intra-class iris templates.

In order to account for rotational inconsistencies, when the Hamming distance of two templates is calculated, one template is shifted left and right bit-wise and a number of Hamming distance values are calculated from successive shifts. This bit-wise shifting in the horizontal direction corresponds to rotation of the original iris region by an angle given by the angular resolution used. If an angular resolution of 180 is used, each shift will correspond to a rotation of 2 degrees in the iris region. This method is suggested by Daugman, and corrects for misalignments in the normalized iris pattern caused by rotational differences during imaging. From the calculated Hamming distance values, only the lowest is taken, since this corresponds to the best match between two templates. The number of bits moved during each shift is given by two times the number of filters used, since each filter will generate two bits of information from one pixel of the normalized region. The actual number of shifts required to normalize rotational inconsistencies will be determined by the maximum angle difference between two images of the same eye, and one shift is defined as one shift to the left, followed by one shift to the right. The shifting process for one shift is illustrated in Figure below.

2.9 Shifting

1. Sometimes a person might move his neck while his eye is photographed. That can cause a shift in the angel axis .
2. To prevent that, shift the matrix cyclic for about 20 columns (which equals to 20 degrees) and try to find the HD not only for the current matrixes but also for all the shifting.
3. the minimal result is the desired one

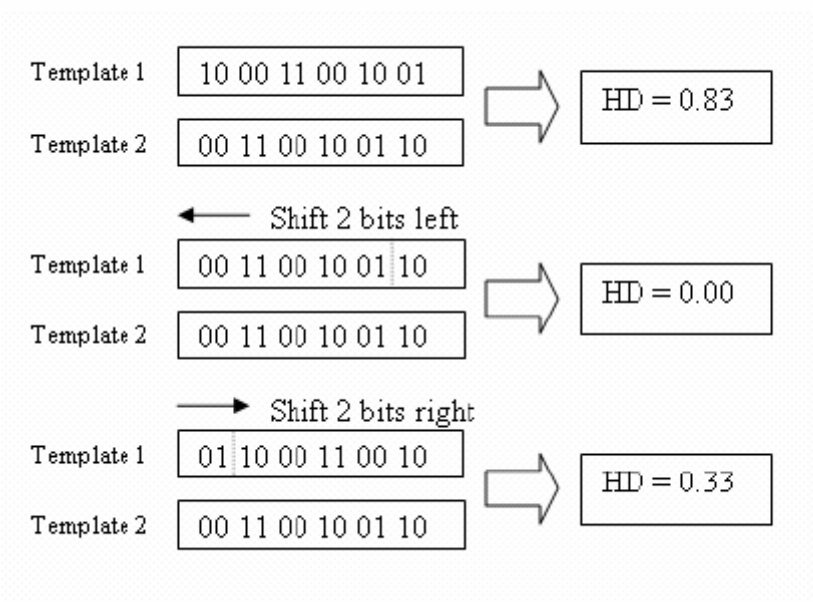

Figure 4-21 An illustration of the shifting process.

One shift is defined as one shift left, and one shift right of a reference template. In this example one filter is used to encode the templates, so only two bits are moved during a shift. The lowest Hamming distance, in this case zero, is then used since this corresponds to the best match between the two templates.

.

5. Results and discussion

Implementation is done in Matlab and the following results have been found. In the first place uniqueness of Iris is routinely and absolutely checked. Primarily this unique iris nature is used to recognize individuals and I got results discussed below. For matching, the Hamming distance was chosen as a metric for recognition, since bit-wise comparisons were necessary. The improved version of Daugman's algorithm is given in the figure5 -3 .

Uniqueness of Iris Patterns: Uniqueness was determined by comparing templates generated from different eyes to each other, and examining the distribution of Hamming distance values produced. This distribution is known as the inter-class distribution.

Uniqueness was also be determined by measuring the number of degrees of freedom represented by the templates. This gives a measure of the complexity of iris patterns, and can be calculated by approximating the collection of inter-class Hamming distance values as a binomial distribution. The number of degrees of freedom, DOF, can be calculated by:

$$DOF = \frac{p(1-p)}{\sigma^2} \tag{5.1}$$

where p is the mean, and σ is the standard deviation of the distribution.

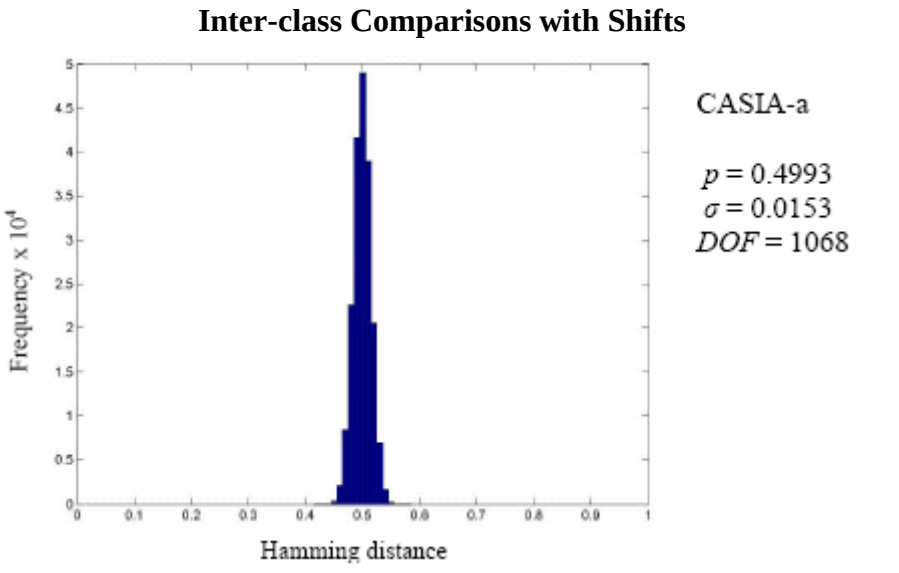

Figure 5.1 – Inter-class Hamming distance distribution of the 'CASIA'

1. The simulation was made for each eye separately. for each eye divide the results into two parts:
    a. Correlation of the same eye (every eye has some pictures).
    b. Correlation of different eyes.
2. The results were also divided to two parts:
    a. Pictures that their Image Processing was perfect.
    b. Pictures that their Image Processing wasn't perfect.

Histogram figures

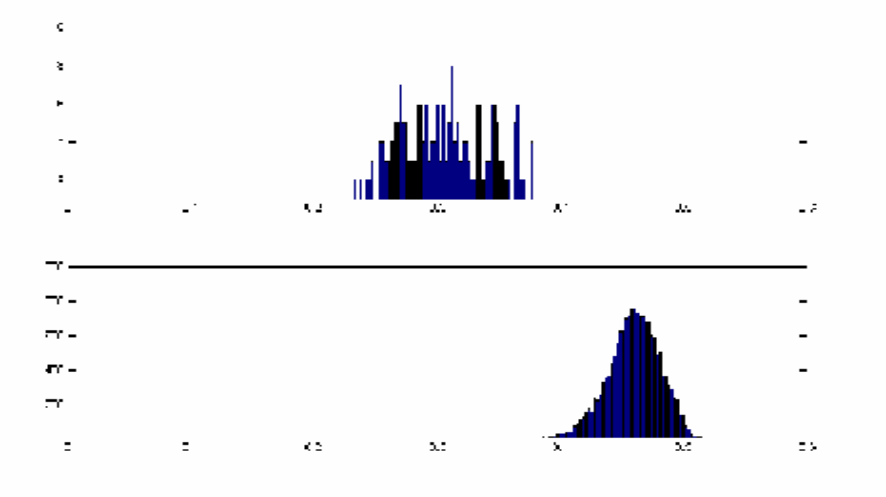

Figure 5-2 The top picture is for the same eyes
The bottom picture is for the different eyes (intra class)

In the Histogram one can see that the average for the same eyes is about 0.3 and the average for the different eyes is about 0.45. But in order to find an absolute threshold I put aside all the bad pictures and by that I get that the minimum HD of the different pictures is more than 0.4 and the maximum HD for the same pictures is less than 0.35. Thus I can choose threshold between 0.35 and 0.4.

Uniqueness was determined by comparing templates generated from different eyes to each other, and examining the distribution of Hamming distance values produced. This distribution is known as the inter-class distribution.

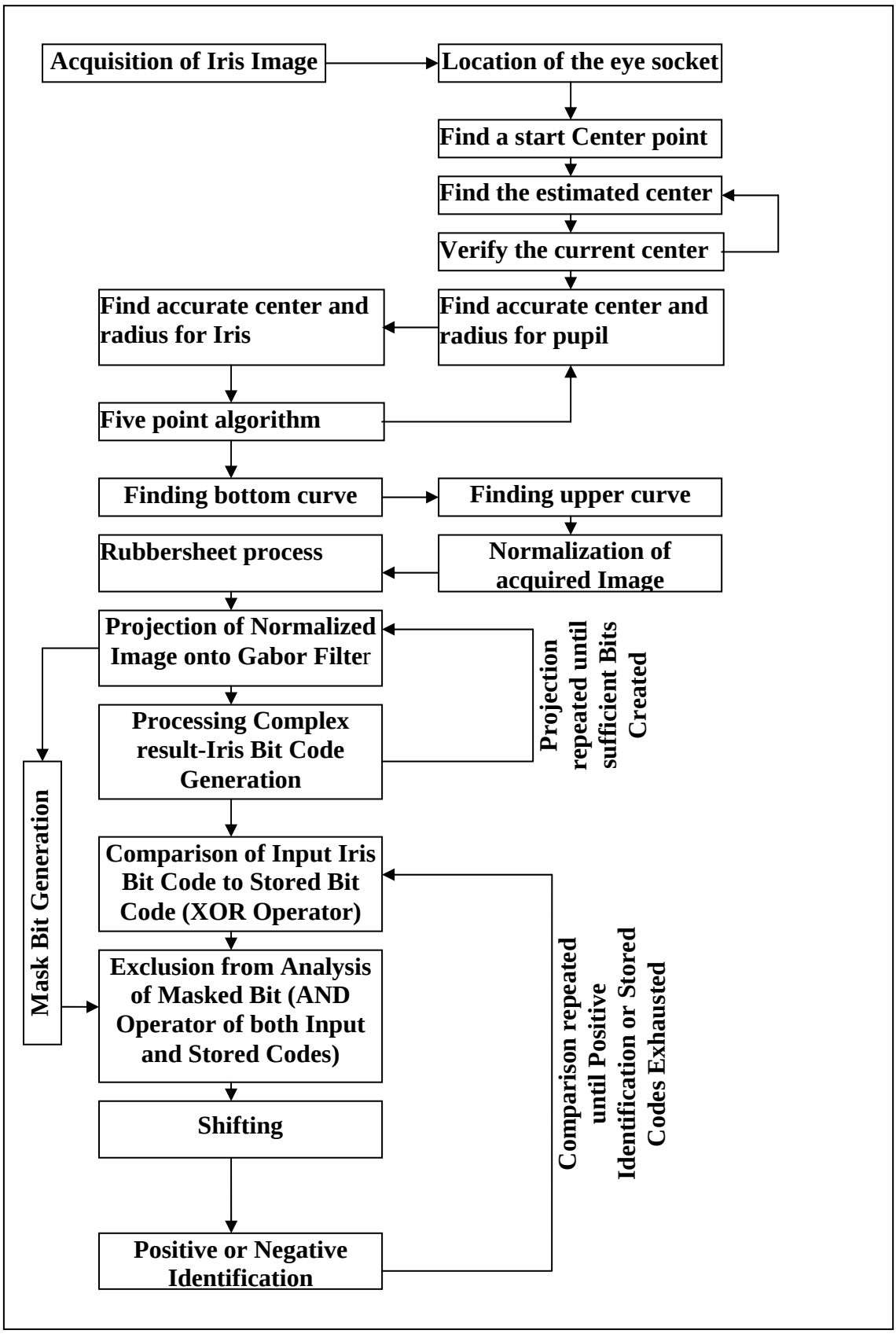

Figure 5-3 General block diagram of improved Daugman's Algorithm

For details of each block diagram look chapter 4 respective sections, where detailed algorithms are given.

6. Conclusion

The original aims of the project were to recreate Daugman's algorithm on iris recognition and improve the system after that.

Daugman's algorithm is separated into 5 different sections. The first section to it finds the location of the iris and pupil. This part further separates into 3 smaller sections. In order to find the size and location of the pupil and iris, an estimated center of the pupil and iris are found in the beginning. After that, the estimated boundaries of the iris and pupil are found using the circular edge detector. The location is then verified to see if it is a good approximation to the center of the iris or the pupil. 8 test points are found to verify if the center point is a good approximation or not. The center is a valid center if more than 7 of the test points are within a certain radius range for the boundary and the intensity change of the boundaries are larger than a threshold value. If it is not a valid center, a new location is found based on the current center. This is done by moving the search location to the direction where most of the valid points are located. If the center of the location remains unchanged, the other matrix that recorded the size of the intensity change will be used. The new location is found by moving the old location to the direction where the highest intensity change is located.

The next section is to normalize the iris image by the rubbersheet method. This is done to reduce the effect of pupil dilation. Gabor filter is then used to extract the iris pattern from the iris image. There is a total of 1024 filters used in the system. The filters are mainly placed on the side closer to the pupil boundary. This is because it is the location where it is rich in pattern. In order to minimize the effect of the noisy region, the locations of the eyelid and eyelash are detected. The reflections on the images are also detected. The reason to detect this region is to mask off the noisy location from comparing. This process is the mask bit generating which is the fourth section of Daugman's algorithm. After finish extracting the data, Hamming distances is used to compare two different irises. If two iris codes have a hamming distance below the threshold value, which is 0.33, it is classified as the same iris code. If not, the iris codes are not different. The first aim of the project is partially successfully.

The final system has a medium processing time with a moderate accuracy. It can only locate around 70-80% of the images from the CASIA database and the recognition rate of those images is around 75%. This is because the localization process has an error rate of about 10 pixels off from the actual center, and this error rate has a big effect on the later processes. The other reason for the low accuracy is because the designs of the filter parameters are based on a small database of size 20. Therefore those 20 images may not have effective representation to all the images in the database. This results in the failure in the mask bit section because the eyelid and eyelash was not effectively removed. As a result, the noisy region was not correctly isolated from the comparing process .This is because they are the regions where most of the noisy regions have occurred. By using this method, it improves the system a bit but not a lot.

However, the second aim of my project, i.e. to extend the system to handle color spectrum images is failed. This is because of a few reasons. Firstly, the iris and pupil detection has a low successful rate. This is because the effect of the reflection dot, the boundary differences for dark eyes are not as clear as the blue eyes. The effect of the reflection has some effect as well. This reflection causes the Gabor filter to fail to encode some components. Another reasons of that is the low resolution of the image, this causes problems on encoding the iris pattern. Finally, the effect of the eyelash and eyelid are not isolated from compare process as well.

7. Future Development

7.1 Filter Design and Localization Improvements

The accuracy of the current system is not as good as it is expected because of the localization and filter parameter problems. There is a limitation on the algorithm to use to detect the location of the iris and the pupil because of the programming environment that is used in the project. As stated before, the development environment is also restricted in the algorithm to use to locate the iris and pupil. Therefore, other method such edge detection than Canny can be used.

The Gabor filter parameters are designed using a small database so that they may be biased. Therefore, the Gabor filter parameters can be improved by using a larger database based to design the parameters. And making Two dimensional Gabor filter.

7.2 Automated Eye Socket Detection

Though I have implemented shifting correcting factor, in order for the system to be commercially used, it must implement as a real time system. The image used in development for this project was using a cut out of the eye image directly, so the location of the eye does not need to take into account throughout the development of this project. However, for a real time system, an image with the whole face is appeared in the image. Therefore, the system must also find the location of the eye socket directly before it can actually start on the iris and pupil detection.

7.3 Real Time System

The current system is not a real time system. It requires images taken at first and stored in database. However, this makes it very inconvenient to use in a real life situation. Therefore, there is a need to improve the system to run with a digital video camera that

will take photo at a specific time period. Therefore, there is no man source required for the system to run and the system is more possible to be used in a real world situation.

7.4 Implementation Using Other Programming Language

The current system is written using Matlab. This is because there are lots of built-in functions and toolbox that makes developing the system much easier. However, there is a major disadvantage for using Matlab. The looping in Matlab programs will take a long time to run and that will slow down the progress dramatically. Therefore, the performance of the program is not very good. However, it needs a long processing time. Therefore, if other algorithm is used in the system, developing in Matlab is not a good choice. Other than implementing the system in other programming language, the performance of the system can be improved by using some special produced hardware. The image quality can be improved by using a customized camera that can capture the iris pattern clearly and minimize the chance of creating noise, such as the reflection caused by the flashlights. Another way to improve the system is to use digital signal processing hardware. This helps to increase the performance and the accuracy of the system.

7.5 Improvements on Color Visible Spectrum Database

Improve the system to handle all kinds of colored Iris image. The number of different races and eye colors are unbalanced. The light source for each image is not constant. The head-tilting angle is not constant. The first improvement is to balance the number of different races and eye colors in order to have a good representation for the database. The lighting source of the database should be constant for each photo. Therefore it is best to set up a fix position to take the photo in. The reflection problem appears in the photo can be solved by avoid the use of flashlights to take the photograph.

References:

[1]Biometrics Consortium, Retrieved from, 2006 http://www.biometrics.org/html/introduction.html

[2] Sanderson S, Authentication For Secure Environments Based On Iris Scanning Technology, et al, IEEE Ref No-00847019

[3] Tisse C., L. Martin, L. Torres, M. Robert. Person identification technique using human iris recognition. *International Conference on Vision Interface*, Canada, 2002.

[4] Daugman, J.G. (1993) High Confidence Recognition of Person by a Test of Statistical Independence. *IEEE Transaction on Pattern analysis and Machine Intelligence*, 15(11), 1148-1161

[5] Woodward, J.D. 1997. Biometrics: privacy's foe or privacy's friend? *Proceedings of the IEEE*, 85 (9), Sep, 1480 -1492.

[6] Liu, S., Silverman, M. 2001. A practical guide to biometric security technology. *IT Professional*, 3 (1) , Jan/Feb, 27 -32

[7] Wayman, J.L. 1997. A generalized biometric identification system model. *Signals, Systems & Computers, 1997. Conference Record of the Thirty-First Asilomar Conference*, 1, 2-5 Nov, 291-295.

[8] Wayman, J.L. 1999. Error rate equations for the general biometric system. *IEEE Robotics & Automation Magazine*, 6 (1), Mar, 35 -48.

[9] Fernando L. Podio, "Biometrics - technologies for highly secure personal authentication", http://csrc.nist.gov/publications/nistbul/itl05-2001.txt

[10] Chellappa, R., Wilson, C.L., Sirohey, S. 1995. "Human and machine recognition of faces: a survey," *Proceedings of the IEEE*, 83 (5), May, 705 -741.

[11] Barrett, W.A. 1997. A survey of face recognition algorithms and testing results. *Signals, Systems & Computers, 1997. Conference Record of the Thirty-First Asilomar Conference*, 1, 2-5 Nov, 301 -305.

[12] Wayman, J.L. 2002. Digital signal processing in biometric identification: a review. *Image Processing. 2002. Proceedings. 2002 International Conference*, 1, I-37 -I-40

[13] Jain, A., Ross, A., Prabhakar, S. 2001. Fingerprint matching using minutiae and texture features. *Image Processing, 2001. Proceedings. 2001 International Conference*, 3, 282 -285.

[14] Prabhakar, S., Jain, A.K., Jianguo Wang, Pankanti, S., Bolle, R. 2000. Minutia verification and classification for fingerprint matching. *Pattern Recognition, 2000. Proceedings. 15th International Conference*, 1, 25 -29.

[15] Huvanandana, S., Changick Kim, Jenq-Neng Hwang. 2000. Reliable and fast fingerprint identification for security applications. *Image Processing, 2000. Proceedings. 2000 International Conference*, 2, 503 -506.

[16] Connell, J.H., Ratha, N.K., Bolle, R.M. 2002. Fingerprint image enhancement using weak models. *Image Processing. 2002. Proceedings. 2002 International Conference*, 1, I-45 -I-48.

[17] Emiroglu, I., Akhan, M.B. 1997. Pre-processing of fingerprint images. *Security and Detection, 1997. ECOS 97., European Conference*, 28-30 Apr, 147 -151.

[18] Xiping Luo, Jie Tian, Yan Wu, 2000. A minutiae matching algorithm in fingerprint verification. *Pattern Recognition, 2000. Proceedings. 15th International Conference*, 4, 833 -836.

[19] Sanchez-Reillo, R., Sanchez-Avila, C., Gonzalez-Marcos, A. 2000. Biometric identification through hand geometry measurements. *Pattern Analysis and Machine Intelligence, IEEE Transactions*, 22 (10), Oct, 1168 -1171.

[20] Sanchez-Reillo, R. 2000. Hand geometry pattern recognition through Gaussian mixture modeling. *Pattern Recognition, 2000. Proceedings. 15th International Conference*, 2, 937 -940.

[21] Cross, J.M., Smith, C.L. 1995. Thermographic imaging of the subcutaneous vascular network of the back of the hand for biometric identification. *Security Technology, 1995. Proceedings. IEEE 29th Annual 1995 International Carnahan Conference*, 18-20 Oct, 20 -35.

[22] Sang Kyun Im, Hyung Man Park, *et. al*. 2001. An biometric identification system by extracting hand vein patterns. *Journal of the Korean Physical Society*. March, 38 (3), 268-72.

[23] Yong Zhu, Tieniu Tan, Yunhong Wang. 2000. Biometric personal identification based on iris patterns. *Proceedings 15th International Conference on Pattern Recognition*. 2, 801-4.

[24] Negin, M., Chmielewski, T.A., Jr., *et. al*. 2000. An iris biometric system for public and personal use. *Computer*, 33 (2), Feb, 70 -75.

[25] de Martin-Roche, D., Sanchez-Avila, C., Sanchez-Reillo, R. 2001. Iris recognition for biometric identification using dyadic wavelet transform zero-crossing. *Security Technology, 2001 IEEE 35th International Carnahan Conference*, Oct, 272 -277.

[26] Daugman, J. 2002. How iris recognition works. *Image Processing. 2002. Proceedings. 2002 International Conference*, 1, I-33 -I-36.

[27] Li Ma, Yunhong Wang, Tieniu Tan. 2002. Iris recognition using circular symmetric filters *Pattern Recognition, 2002. Proceedings. 16th International Conference*, 2, 414 -417.

[28] Podio, F.L. 2002. Personal authentication through biometric technologies. *Networked Appliances, 2002. Proceedings. 2002 IEEE 4th International Workshop*, 57 - 66.

[29] The Biometric White Paper, Julian Ashboum, Avanti site: http://homepage.ntlworld.com/avanti/

[30] Xiaoyi Jiang, Mojon, D. 2003. Adaptive local thresholding by verification-based multithreshold probing with application to vessel detection in retinal images. *Pattern Analysis and Machine Intelligence, IEEE Transactions*, 25(1), 131 -137.

[31] Camino, J.L., Travieso, C.M., Morales, C.R., Ferrer, M.A. 1999. Signature classification by hidden Markov model. *Security Technology, 1999. Proceedings. IEEE 33rd Annual 1999 International Carnahan Conference*, 481 -484.

[32] Vergara da Silva, A., Santana de Freitas, D. 2002. Wavelet-based compared to function-based on-line signature verification. *Computer Graphics and Image Processing, 2002. Proceedings. XV Brazilian Symposium*, 218 -225.

[33] Lin Hong; Anil Jain. 1998. Integrating faces and fingerprints for personal identification. *Pattern Analysis and Machine Intelligence, IEEE Transactions*, 20(12), Dec, 1295 -1307.

[34] Jain, A.K., Ross, A. 2002. Learning user-specific parameters in a multibiometric system. *Image Processing. 2002. Proceedings. 2002 International Conference*, 1, I-57 - I-60.

[35] Dugelay, J.L., Junqua, J.C., Kotropoulos, C., Kuhn, R., Perronnin, F., Pitas, I. 2002. Recent advances in biometric person authentication. *Acoustics, Speech, and Signal Processing, 2002 IEEE International Conference*, 4, IV-4060 -IV-4063.

[36] Osadciw, L., Varshney, P., Veeramachaneni, K. 2002. Improving personal identification accuracy using multisensor fusion for building access control applications.

Information Fusion, 2002. Proceedings of the Fifth International Conference, 2, 1176 - 1183.

[37] Kittler, J., Messer, K. 2002. Fusion of multiple experts in multimodal biometric personal identity verification systems. *Neural Networks for Signal Processing, 2002. Proceedings of the 2002 12th IEEE Workshop*, 3 -12.

[38] Pankanti, S., Bolle, R.M., Jain A. 2000. Biometrics: The Future of Identification. *Computer*, 33 (2), Feb, 46 -49

[39] Masek, L. (2003) *Recognition of Human Iris Pattern for Biometric Identification.* The School of Computer Science and Software Engineering, University of Western Australia

[40] Individual Biometrics. Retrieved from http://ctl.ncsc.dni.us/biomet%20web/BMIris.html

[41] Albrecht A. Biometrics and consumer protection. Retrieved From http://www.vzbv.de/go/dokumentepositionen/45/1/4

[42] Biometric FAQ. Retrieved from http://www.bromba.com/faq/biofaqe.htm#vom%20Anwender

[43] Python vs Perl vs Java vs C++. Retrieved from http://www.flat222.org/mac/bench/

[44] Java VS c++. Retrieved from http://www.cs.wustl.edu/~levine/courses/cs342/c++/javaVcpp-index.html

[45] S. Sanderson, J. Erbetta. Authentication for secure environments based on iris scanning technology. IEE Colloquium on Visual Biometrics, 2000.

[46] R. Wildes. Iris recognition: an emerging biometric technology. Proceedings of the IEEE, Vol. 85, No. 9, 1997.

[47] R. Wildes, J. Asmuth, G. Green, S. Hsu, R. Kolczynski, J. Matey, S. McBride. A system for automated iris recognition. Proceedings IEEE Workshop on Applications of Computer Vision, Sarasota, FL, pp. 121-128, 1994.

[48] W. Boles, B. Boashash. A human identification technique using images of the iris and wavelet transform. IEEE Transactions on Signal Processing, Vol. 46, No. 4, 1998.

[49] S. Lim, K. Lee, O. Byeon, T. Kim. Efficient iris recognition through improvement of feature vector and classifier. ETRI Journal, Vol. 23, No. 2, Korea, 2001.

[50] Daugman, J (2003). The importance of being random: Statistical principles of iris recognition. Pattern Recognition, Vol 36, No. 2, Pgs 279-291

[51] Daugman, J (2003). Demodulation by complex-valued Wavelets for stochastic pattern Recognition. International Journal of wavelets, Multiresolution and Information processing, vol.1 No. 1, pgs 1-17.

[52]Jones, C (2003). Color face Recognition Using Quaternoinic Gabor filters, retrieved from http://filebox.vt.edu/users/crjones4/

[53]Umeyama, S (2003). Blind Deconvolution of Image Using Gabor Filters and Independent Component Analysis and Blind Signal Separation (ICA2003), pgs 319-324.

[54] CASIA- Chinese Academy of Sciences – Institute of Automation. Database of 756 Greyscale Eye Images. http://www.sinobiometrics.com Version 1.0, 2003.

[55] Universidade da Beira Interior, Departamento de Informática Database of 1877 colored iris pictures retrieved with permission from UBIRIS http://iris.di.ubi.pt/